the plant journal

SEB SOCIETY FOR EXPERIMENTAL BIOLOGY

The Plant Journal (2020) doi: 10.1111/tpj.15057

Ectopic overexpression of a membrane-tethered transcription factor gene *NAC60* from oilseed rape positively modulates programmed cell death and age-triggered leaf senescence

Jingli Yan[1,†], Qinqin Chen[1], Xing Cui[1], Peiyu Zhao[1], Shidong Gao[1], Bo Yang[1,*], Jian-Xiang Liu[2], Tiantian Tong[1], Michael K. Deyholos[3] and Yuan-Qing Jiang[1,*]

[1]*State Key Laboratory of Crop Stress Biology for Arid Areas, College of Life Sciences, Northwest A & F University, Yangling, Shaanxi 712100, China,*

[2]*State Key Laboratory of Plant Physiology and Biochemistry, College of Life Sciences, Zhejiang University, Hangzhou, Zhejiang 310027, China, and*

[3]*Department of Biology, University of British Columbia, Okanagan Campus, Kelowna, BC V1V 1V7, Canada*

Received 23 September 2019; revised 8 July 2020; accepted 13 July 2020.

*For correspondence (e-mail yangwl@nwafu.edu.cn; jiangyq@nwafu.edu.cn).

†Present address: College of Plant Protection, Henan Agricultural University, Zhengzhou, 450002, Henan, China

SUMMARY

Senescence is an integrative final stage of plant development that is governed by internal and external cues. The NAM, ATAF1/2, CUC2 (NAC) transcription factor (TF) family is specific to plants and membrane-tethered NAC TFs (MTTFs) constitute a unique and sophisticated mechanism in stress responses and development. However, the function of MTTFs in oilseed rape (*Brassica napus* L.) remains unknown. Here, we report that BnaNAC60 is an MTTF associated with the endoplasmic reticulum (ER) membrane. Expression of *BnaNAC60* was induced during the progression of leaf senescence. Translocation of BnaNAC60 into nuclei was induced by ER stress and oxidative stress treatments. It binds to the NTLBS motif, rather than the canonical NAC recognition site. Overexpression of *BnaNAC60* devoid of the transmembrane domain, but not the full-length *BnaNAC60,* induces significant reactive oxygen species (ROS) accumulation and hypersensitive response-like cell death in both tobacco (*Nicotiana benthamiana*) and oilseed rape protoplasts. Moreover, ectopic overexpression of *BnaNAC60* devoid of the transmembrane domain, but not the full-length *BnaNAC60*, in Arabidopsis also induces precocious leaf senescence. Furthermore, screening and expression profiling identified an array of functional genes that are significantly induced by *BnaNAC60* expression. Further it was found that BnaNAC60 can activate the promoter activities of *BnaNYC1*, *BnaRbohD*, *BnaBFN1*, *BnaZAT12*, and multiple *BnaVPEs* in a dual-luciferase reporter assay. Electrophoretic mobility shift assay and chromatin immunoprecipitation coupled to quantitative PCR assays revealed that BnaNAC60 directly binds to the promoter regions of these downstream target genes. To summarize, our data show that BnaNAC60 is an MTTF that modulates cell death, ROS accumulation, and leaf senescence.

Keywords: NAC transcription factor, programmed cell death, leaf senescence, oilseed rape, reactive oxygen species.

INTRODUCTION

Leaf senescence is the last stage of leaf development and is characterized by leaf yellowing and massive programmed cell death (PCD) (Thomas, 2013). Leaf senescence plays an important role in crop yield determination as many nutrients are relocated from senescent leaves to young leaves or storage organs (Woo *et al.*, 2013). Leaf senescence is not only influenced by endogenous factors such as age, but also by various environmental stresses (Lim *et al.*, 2007). During senescence, leaf cells carry out orderly changes in cell structure, metabolism, and gene expression, including degradation of proteins, membrane lipids, and nucleic acid (Lim *et al.*, 2007). The most obvious phenotype in aging plants is yellow leaves caused by the degradation of chlorophyll (Hortensteiner, 2006). Some chlorophyll catabolic genes (CCGs) have been identified in the last decade or so, such as *NYC1* (*Non-Yellow Coloring 1*, which encodes a Chl b reductase) and *SGR1 (Stay Green 1*, also known as *NYE1*, *Non-Yellowing 1*), which are critical regulators of

chlorophyll degradation (Sato *et al.*, 2009). Besides chlorophylls, leaf senescence is also induced by increased expression of different enzymes that hydrolyze many other macromolecules (Lim *et al.*, 2007). Genes encoding these catabolic enzymes, along with many other genes coding for proteins implicated in nutrient recycling, are among the hundreds of senescence-associated genes (SAGs) that are induced during senescence (Gan and Amasino, 1997; He and Gan, 2002; Gepstein *et al.*, 2003; Guo *et al.*, 2004). For instance, *AtSAG12* encodes a cysteine protease involved in nitrogen mobilization during senescence (James *et al.*, 2018). *AtSAG13* encodes a short-chain alcohol dehydrogenase (Weaver *et al.*, 1998). *AtSAG29* codes for a sugar transporter of the SWEET family (Seo *et al.*, 2011), whereas *AtSAG113* encodes a clade A protein phosphatase type 2C (PP2C) (Zhang and Gan, 2012),

A few studies have shown that developmental senescence is also associated with increased reactive oxygen species (ROS) levels, which not only assist in degradation of cellular components for recycling but also play signaling roles in initiating the senescence process (Guo and Gan, 2012; Rogers and Munne-Bosch, 2016; Yang *et al.*, 2018). Hydrogen peroxide (H_2O_2) is a major form of ROS involved in senescence, with ROS being the main by-products of photosynthesis and respiration or other metabolic processes (Mittler, 2017). Respiratory burst oxidase homolog (RBOH) proteins are the major enzymes responsible for ROS production in the apoplast (Suzuki *et al.*, 2011). ROS are tightly linked with both leaf senescence and PCD and positively influence these two processes (Mhamdi and Van Breusegem, 2018). In plants, there are two types of PCD, with one being developmental PCD occurring in the vegetative and reproductive developmental processes and the other being environmental stress-induced PCD (Daneva *et al.*, 2016). Although sometimes used interchangeably, leaf senescence shows a difference from PCD (Buono *et al.*, 2019). Whereas nutrient remobilization is an active cellular program depending on the viability of nuclei and mitochondria, PCD marks the endpoint of the senescence process (Thomas, 2013). At the final stage of leaf senescence, PCD is a typical symptom resulting from the disintegration of plasma and vacuolar membranes (Daneva *et al.*, 2016). Upon the rupture of the tonoplast, hydrolytic enzymes including vacuolar processing enzymes (VPEs) are released into the cytoplasm. VPEs are evolutionarily related to and share structural homology with animal caspases and play an important role in PCD (Hatsugai *et al.*, 2004). Both PCD and leaf senescence need to be tightly coordinated and controlled to optimize recuperation of nutrients. However, the transcriptional control of key genes involved in these two processes remains unknown for oilseed rape (*Brassica napus* L.).

Previous studies have demonstrated that many genes are induced during the progress of leaf senescence in Arabidopsis (*Arabidopsis thaliana*) (Gepstein *et al.*, 2003; Guo *et al.*, 2004; Woo *et al.*, 2016), which include those encoding transcription factors (TFs) of the WRKY and NAC families (Balazadeh *et al.*, 2008; Kim *et al.*, 2016). The NAC (No Apical Meristem, NAM; Arabidopsis Transcription Activation Factor, ATAF; Cup-shaped Cotyledon, CUC) proteins constitute a large family of plant-specific TFs (Olsen *et al.*, 2005). A total of 113 and 140 NAC genes have been identified from Arabidopsis and rice (*Oryza sativa*), respectively, which code for proteins which share a conserved DNA-binding NAC domain at the N-terminus, whereas the C-terminal sequences are relatively divergent and contain a potential transcriptional regulatory domain (Puranik *et al.*, 2012). A few NAC TFs are found to play important roles in regulating leaf senescence and under some circumstances two or three NACs work together to modulate the same senescence process (Balazadeh *et al.*, 2008; Kim *et al.*, 2016). For instance, ANAC092 (also referred to as ORESARA1, ORE1), AtNAP (ANAC029), ANAC059 (also referred to as ORE1 Sister 1, ORS1), and ANAC016 are positive regulators of leaf senescence (Guo and Gan, 2006; Balazadeh *et al.*, 2010, 2011; Kim *et al.*, 2013; Sakuraba *et al.*, 2015, 2016). ORE1 could directly activate *CCG* expression and repress the expression of *Golden2-Like 2* (*GLK2*) to accelerate the leaf senescence process (Rauf *et al.*, 2013; Qiu *et al.*, 2015). Moreover, ORE1 interacts with and activates the promoter of *Bifunctional Nuclease 1* (*BFN1*), whose encoded protein modulates nucleic acid breakdown during senescence and PCD (Perez-Amador *et al.*, 2000). JUNGBRUNNEN1 (JUB1 also referred to as ANAC042) and VND-Interacting 2 (VNI2, also referred to as ANAC083) are two negative regulators in leaf senescence, and *JUB1* expression can be induced by H_2O_2 (Yang *et al.*, 2011; Wu *et al.*, 2012). Moreover, it has been reported that NAC TFs also modulate the senescence process in crops such as rice (Liang *et al.*, 2014; Mao *et al.*, 2017), tomato (*Solanum lycopersicum*) (Ma *et al.*, 2018), soybean (*Glycine max*) (Pimenta *et al.*, 2016), and wheat (*Triticum*) (Uauy *et al.*, 2006), which ultimately influence the yield. In addition, soybean NAC30 and NAC81 modulate endoplasmic reticulum (ER) and osmotic stress, and induce cell death through a group of VPEs (Mendes *et al.*, 2013). *VPEs* encode cysteine proteinases and have caspase-1-like activities in plants (Hatsugai *et al.*, 2015). However, no such TF has been identified from oilseed rape.

Among the NAC TFs in higher plants, a few members possess transmembrane domains (TDs) at their C-termini, which are called NAC with transmembrane motif 1 (NTM1) or NTM1-like (NTLs) (Kim *et al.*, 2006, 2007). AtNTLs may be associated with the ER or the nuclear membrane (Liang *et al.*, 2015). NTLs are proposed to possess an intriguing activation strategy to ensure rapid transcriptional responses to various stimuli through proteolytic cleavage of TDs (Chen *et al.*, 2008). There are approximately 18 *NTLs*

in Arabidopsis and five *NTLs* in rice (Kim *et al.*, 2007, 2010b). *NTLs* have also been identified in other crop plants, including oilseed rape (Le *et al.*, 2011; Wang *et al.*, 2015). It is found that most of the AtNTL genes are induced by abiotic stress, which may also mediate their proteolytic cleavage and nuclear translocation (Kim *et al.*, 2006, 2007, 2012; Park *et al.*, 2011). Recently, several NTLs have been reported to be involved in either mitochondrial retrograde signaling (De Clercq *et al.*, 2013; Ng *et al.*, 2013; Van Aken and Pogson, 2017), the unfolded protein response (UPR) (Yang *et al.*, 2014a), or ER-stress-induced PCD (Yang *et al.*, 2014b). However, the function of NTLs in oilseed rape remains unknown.

We previously identified and cloned as many NAC genes as possible from oilseed rape, among which a few encode NTLs (Wang *et al.*, 2015). Here, we report the functional characterization of BnaNAC60, a membrane-tethered NAC TF that positively modulates cell death, ROS accumulation, and leaf senescence, likely through regulating the transcription of downstream target genes directly implicated in these processes.

RESULTS

BnaNAC60 encodes a membrane-tethered transcription factor and its expression is induced in senescing leaves

Previously, more than 10 NTL genes were cloned from oilseed rape through reverse transcription PCR (RT-PCR). *BnaNAC60* was named as it shows the highest similarity to *ANAC060* (At3g44290) among all *ANACs* in Arabidopsis. Further, *BnaNAC60* was mapped onto the C subgenome with the locus number being BnaC01g23890D in the *B. napus* genome. *BnaNAC60* is predicted to encode a protein of 340 amino acid residues, which contains a conserved NAC domain divided into five subdomains (A–E) and a putative transmembrane domain at its C-terminus (Figure 1a; Figure S1). However, BnaNAC60 is also different from ANAC060 from Col-0 in that ANAC060 from Col-0 has no predicted transmembrane domain (Figure S1). This difference is caused by a single-nucleotide polymorphism in Col-0 *ANAC060*, which affects its splicing pattern (Li *et al.*, 2014). Therefore, we explored the function and underlying mechanism of *BnaNAC60*. A phylogenetic analysis of NTLs from representative plant species showed that BnaNAC60 is very closely related to ANAC089 (NTL17) and ANAC040 (NTL8), belonging to subclade IV (Figure S2). Among the five OsNTLs, BnaNAC60 shows the highest similarity to OsNTL3 (ONAC074, Os01g15640), the function of which has not been reported. Interestingly, we did not identify any NTL gene in moss (*Physcomitrella patens*, bryophyte) and spike moss (*Selaginella moellendorffii*, lycophyte), two species of special importance for the study of plant evolution. *Physcomitrella patens* is a non-vascular plant while *S. moellendorffii* is thought to be the earliest evolved extant vascular land plant (Bowman *et al.*, 2007). The absence of *NTLs* in these two moss plants suggests *NTLs* may exist in higher land plants only.

In order to investigate the subcellular localization of BnaNAC60, its full-length coding region (1–340 amino acids [aa]) and a truncated fragment devoid of the putative transmembrane domain *BnaNAC60ΔTM* (1–321 aa) were fused downstream of *GFP* (encoding green fluorescent protein), which was expressed under the control of the cauliflower mosaic virus (CaMV) 35S promoter in leaf cells of *Nicotiana benthamiana*. The HDEL-mCherry and nuclear localization sequence (NLS)-mCherry cassettes were co-expressed to indicate the ER and nuclei, respectively. The results showed that most of the GFP-BnaNAC60 signals were observed in the ER, overlapping with those of HDEL-mCherry, while the GFP-BnaNAC60ΔTM signals were distributed exclusively in nuclei, overlapping completely with those of NLS-mCherry (Figure 1b). These results suggest that BnaNAC60 is a membrane-tethered TF, and the full-length protein is an inactive or dormant form, while the truncated form devoid of the transmembrane domain functions in the nucleus. In this aspect, BnaNAC60 is very different from its ortholog in Arabidopsis Col-0, which has no transmembrane domain at all and is targeted to nuclei only (Figure S3) (Liang *et al.*, 2015).

It has been reported that ANAC089 is an MTTF and that its translocation from the membrane to the nucleus is induced by ER stress (Yang *et al.*, 2014b). BnaNAC60 is phylogenetically close to BnaNAC089 and ANAC089 (Figure S2). We therefore considered whether BnaNAC60ΔTM could form a heterodimer with BnaNAC89ΔTM *in vivo*. The results showed that BnaNAC60ΔTM interacts with BnaNAC89ΔTM in nuclei (Figure S4).

Translocation of BnaNAC60 was induced by ER stress and oxidative stress treatments

To investigate whether the translocation of BnaNAC60 was induced by ER stress or oxidative stress treatment, *GFP-BnaNAC60*, *GFP*, and *GFP-ANAC089* were individually transiently expressed in oilseed rape protoplasts. Among these, *GFP* was used a negative control, while *GFP-ANAC089* was set up as a positive control. Tunicamycin (Tn) and H_2O_2 were used to induce ER stress and oxidative stress, respectively. The results showed that GFP alone did not show any change after Tn treatment and displayed a cytosolic–nuclear distribution as expected (Figure S6a,b). In the mock-treated protoplasts, most of the GFP-BnaNAC60 signals overlapped with those of the ER marker (Figure S6c). After treatment with Tn, green fluorescence signals emitted by GFP-BnaNAC60 were largely found in the nuclei (Figure S6d). The positive control GFP-ANAC089 showed a similar change (Figure S4e,f), which is consistent with the previous report (Yang *et al.*, 2014b). Moreover, the

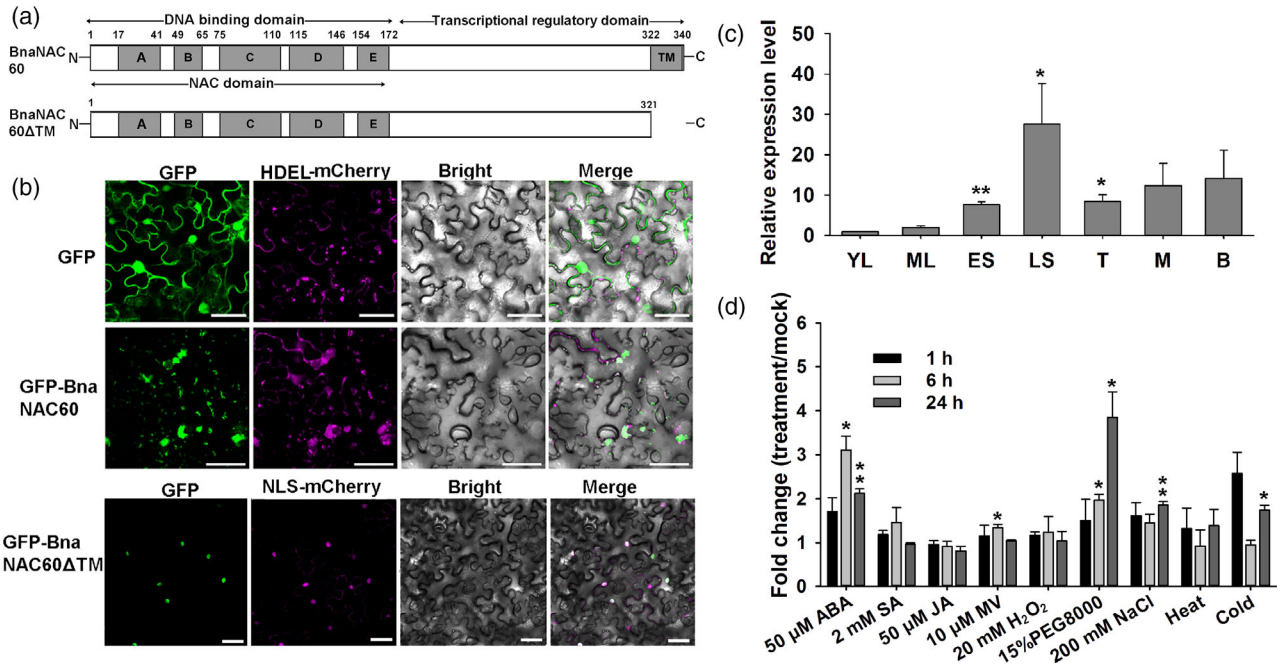

Figure 1. Subcellular localization of BnaNAC60 and expression analysis of *BnaNAC60*. (a) Schematic representation of the BnaNAC60 protein. The N-terminus contains a conserved NAC domain which can be divided into five subdomains and has DNA-binding ability. The C-terminus has transcriptional regulatory ability and contains a transmembrane domain. BnaNAC60ΔTM is a truncated form without the transmembrane domain. (b) Subcellullar localization of BnaNAC60 and its truncated form by transient expression in *N. benthamiana* cells. The GFP-BnaNAC60 and GFP-BnaNAC60ΔTM fusion proteins were co-localized with the mCherry-tagged HDEL or the NLS. Bar, 50 μm. (c) Expression levels of *BnaNAC60* as determined by qRT-PCR during leaf development in oilseed rape. The fourth true leaves of oilseed rape at different developmental stages were used for the assay. YL, young leaves; ML, mature leaves; ES, early senescent leaves; LS, late senescent leaves; T, M, and B are the tip, middle, and base of ES leaves. (d) Expression of *BnaNAC60* upon various treatments including 50 μM (±)-ABA, 2 mMsalicylic acid (SA), 50 μM JA, 10 μM methyl viologen (MV), 20 mM H_2O_2, 15% PEG8000, 200 mM NaCl, heat (38°C), and cold (4°C). In (c,d), data represent means of three biological replicates ± SE compared to YL (c) or mock treatment (d). Asterisks indicate significant differences by Student's *t*-test (*$P \leq 0.05$; **$P \leq 0.01$).

expression of some known ER stress-related genes, including *Binding Protein* (*BiP*), *Calnexin 1* (*CNX1*), and *Protein Disulfide Isomerase* (*PDI*), were significantly induced in protoplasts transfected with *BnaNAC60* compared with *GFP* upon ER stress treatment (Figure S6). In addition, translocation of BnaNAC60 was also induced by 10 mM H_2O_2 treatment and a longer duration of treatment rendered a complete nuclear localization of BnaNAC60 (Figure S7).

To further explore the function of *BnaNAC60*, we analyzed its transcript levels during leaf development as well as upon stress or hormone treatments through quantitative RT-PCR (qRT-PCR). The results showed that *BnaNAC60* was significantly induced in early senescent leaves and its expression was even higher in late senescent leaves compared with young and mature leaves (Figure 1c). The expression profiling analysis under various treatments showed that *BnaNAC60* expression was significantly induced by abscisic acid (ABA), polyethylene glycol 8000 (PEG8000), salt, methyl viologen (MV), and cold (4°C) treatments at the 6 and/or 24 h time points; no significant difference was detected upon the other treatments (Figure 1d).

BnaNAC60 positively modulates PCD in tobacco

To investigate the function of *BnaNAC60*, we transiently overexpressed it in *N. benthamiana* leaves with *uidA* (encoding β-glucuronidase [GUS]) as the control. We found that expression of *BnaNAC60ΔTM* led to hypersensitive response (HR)-like cell death symptoms as early as 3 days post-infiltration (dpi), and the symptoms were more evident at 5 and 7 dpi (Figure S8a). In contrast, *BnaNAC60* expression showed a mild phenotype only. The HR is a plant defense response triggered by pathogen infection, which results in rapid cell death at the site of pathogen ingress and thus confines the spreading of pathogens to distal parts of plants. HR is also a form of PCD that can activate defense for attenuating subsequent attacks (Heath, 2000). Since HR-like cell death is associated with ROS, we performed 3,3′-diaminobenzidine (DAB) staining and a quantitative assay of H_2O_2 content. It was found that there was more H_2O_2 accumulation in *BnaNAC60*- and *BnaNAC60ΔTM*-expressing tissues than in GUS controls, while *BnaNAC60ΔTM* expression had a more prominent effect than *BnaNAC60* (Figure S8b). Malonaldehyde (MDA) is an important indicator of lipid peroxidation as a result of ROS

accumulation. Our data showed that the content of MDA in leaf tissues expressing *BnaNAC60ΔTM* was higher than in the GUS control from 5 dpi, while *BnaNAC60* expression led to significantly more MDA until 7 dpi (Figure S8c). Furthermore, an increase in ion leakage in tissues overexpressing *BnaNAC60ΔTM* was detected, which reflected the extent of cell death (Figure S8d). Moreover, loss of chlorophyll and production of anthocyanins were detected since they are central indicators in senescing leaves. The concentration of chlorophyll in leaf tissues expressing *BnaNAC60ΔTM* decreased significantly after 5 dpi, while the content of anthocyanins significantly increased, whereas the expression of *BnaNAC60* caused a more slow and mild change (Figure S8e,f). To substantiate the hypothesis that the *BnaNAC60*-induced leaf senescence was associated with PCD, we employed a terminal deoxynucleotidyl transferase dUTP nick end labeling (TUNEL) assay. The results showed there were evident green signals emitted from fluorescein isothiocyanate (FITC)-labeled nuclear DNA ends from *BnaNAC60*- and *BnaNAC60ΔTM*-expressing tissues, with more signals detected in the latter than in the former. In contrast, no signal was detected in GUS-expressing tissues (Figure S9).

Interestingly, ectopic overexpression of *ANAC060* from Col-0 in tobacco leaves failed to induce cell death symptoms and ROS production (Figure S10a), and no significant difference in chlorophyll content and relative conductivity was observed between tissues overexpressing *ANAC060* and the GFP control (Figure S10b,c). Moreover, ectopic overexpression of full-length *ANAC060* or *ANAC060ΔTM* from the C24 ecotype in tobacco leaves failed to induce any obvious symptom (Figure S11). However, we found that ectopic overexpression of *ANAC089ΔTM*, but not full-length *ANAC089*, in tobacco leaves induced HR-like cell death symptoms, caused chlorophyll degradation, and increased relative conductivity (Figure S12).

BnaNAC60 positively modulates leaf senescence in Arabidopsis

Next, we expressed *BnaNAC60ΔTM* in Arabidopsis plants under the driving of a constitutive CaMV35S promoter. Transgenic plants expressing *GFP* were prepared at the same time and were used as the control. Two independent homozygous transgenic overexpression lines (OE-28# and OE-31#) were selected from over 30 independent lines for further analyses. qRT-PCR analysis showed that *BnaNAC60ΔTM* levels in the OE-28# and OE-31# lines were increased approximately 1300- and 500-fold, respectively, compared to the GFP control (Figure S13a). Western blot analysis showed that BnaNAC60ΔTM protein was successfully expressed in these two overexpression lines (Figure S13b). The OE-28# and OE-31# lines showed accelerated leaf senescence compared with the *GFP* control line under normal growth conditions at 35 and 40 days post-stratification (dps) (Figure 2a; Figure S13c). No significant difference in flowering time was observed in *BnaNAC60ΔTM*-overexpressing plants, though ANAC089ΔC-overexpressing plants show a delayed flowering phenotype (Li *et al.*, 2010). We also examined the levels of H_2O_2 by DAB staining and quantitative measurement. Rosette leaves of these two OE lines were more strongly stained than those of the control plant (Figure 2a). A quantitative assay of H_2O_2 contents also supported this (Figure 2b). During the process of leaf senescence, loss of chlorophyll and an increase in ion leakage are two typical physiological features. Rates of chlorophyll loss were faster in the OE-28# and OE-31# lines compared with the control (Figure 2c). Moreover, these two OE lines also showed increased ion leakage at both 35 and 40 dps (Figure 2d).

Moreover, full-length *BnaNAC60* was constitutively expressed in Arabidopsis plants driven by the CaMV35S promoter as well. Two independent homozygous transgenic overexpression lines (OE-14# and OE-26#) were selected for the phenotypic analysis. The successful expression of *BnaNAC60* was confirmed in these two OE lines by qRT-PCR and immunoblotting (Figure S14a,b). A phenotypic assay showed that there was no significant difference between the *GFP* control plant and *BnaNAC60* overexpression lines in either 35- or 40-day-old plants (Figure S14c). The chlorophyll content and relative conductivity were also similar among these lines (Figure S14d,e).

We also examined the leaf senescence phenotype of these *BnaNAC60*-OE lines in comparison with control, under dark treatment. To do this, age-matched mature rosette leaves were covered with aluminium foil for dark treatment and the plants were kept under normal growth conditions for 2 or 4 days. The results showed that the *BnaNAC60ΔTM*-OE lines OE-28# and OE-31# showed earlier senescence than the control plants after dark treatment (Figure S15a,c), whereas the *BnaNAC60*-overexpressing lines OE-14# and OE-26# did not show any significant difference compared with the control plants (Figure S15b,d).

Since the *BnaNAC60ΔTM*-OE lines in Arabidopsis showed a precocious leaf senescence phenotype and ROS accumulation, we analyzed the expression of an array of marker genes related to chlorophyll degradation, ROS production, cell death, and senescence. qRT-PCR was performed with rosette leaves of OE-28# and OE-31# lines as well as the control *GFP* transgenic line at 40 dps. The results showed that *AtSAG12* was highly induced in these two overexpression lines; *AtSAG13* was significantly induced in OE-31#; *AtSAG113* was also significantly induced in the two overexpression lines, whereas *AtSAG29* showed no significant increase in the two OE lines (Figure 2e). *AtNYC1* expression was increased twofold, consistent with the loss of chlorophyll in these two OE lines. Moreover, *AtRbohD* and *AtRbohF*, which are responsible for apoplastic ROS production (Marino *et al.*, 2012), were

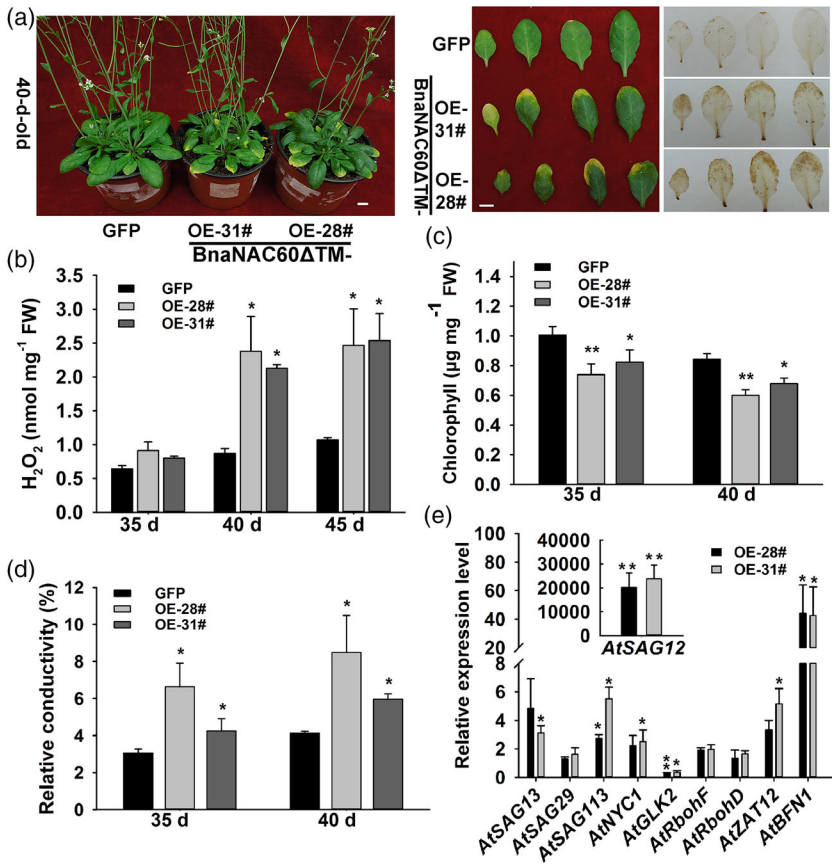

Figure 2. Overexpression of *BnaNAC60ΔTM* in Arabidopsis promotes age-dependent leaf senescence. (a) Phenotype of two *BnaNAC60ΔTM* overexpression lines OE-31# and OE-28# compared to the transgenic *GFP* control line. Photographs were taken at 40 days post-stratification (dps) and the 5th to 8th true leaves were stained with DAB. Bar, 1 cm. (b–d) Quantification of H_2O_2 content (b), chlorophyll content (c), and relative conductivity (d) in these two OE lines compared with the control line. Values represent the means of three independent replicates ± SE. Asterisks indicate significant differences compared to the *GFP* control line by Student's *t*-test (*$P \leq 0.05$; **$P \leq 0.01$). (e) qRT-PCR analysis of the expression of senescence-, ROS-, and cell death-related marker genes in these two OE lines at 40 dps. Age-matched plants of the *GFP* line were used as the control. Data are presented as the mean of three replicates ± SE. Asterisks indicate significant differences compared to the expression levels in the *GFP* control line by Student's *t*-test (*$P \leq 0.05$; **$P \leq 0.01$).

also induced, though the magnitude was not large. *AtZAT12*, encoding a zinc finger TF involved in ROS metabolism (Davletova *et al.*, 2005), was significantly induced in OE-31#. *AtBFN1*, encoding a bifunctional nuclease involved in nucleic acid degradation and leaf senescence (Perez-Amador *et al.*, 2000), was significantly induced (Figure 2e). In contrast, *AtGLK2*, encoding a TF positively regulating chloroplast development (Waters *et al.*, 2008), was significantly repressed in these two OE lines (Figure 2e). The transcript abundance of these marker genes in *BnaNAC60* overexpression lines OE-14# and OE-26# was analyzed as well. It can be seen that most of these marker genes showed no significant change, though *AtSAG12*, *AtSAG13*, *AtZAT12*, and *AtBFN1* were slightly induced (Figure S14f).

BnaNAC60 modulates cell death and ROS accumulation in oilseed rape

To explore the function of *BnaNAC60* in oilseed rape, both the full-length *BnaNAC60* and *BnaNAC60ΔTM* were transiently expressed in protoplasts of oilseed rape, which is a rapid and efficient system to study the function of a gene (Kaneda *et al.*, 2009). Plasmids expressing *GFP* or *uidA* were used as controls. To confirm these genes were successfully expressed in protoplasts, we observed the GFP fluorescence and detected their abundance by immunoblotting assay. The results were all as expected (Figure S16a,b). We subjected the transfected protoplasts to various stainings. Firstly, live cells cannot be stained by Evans blue, and only dead cells can be stained with dark-blue color. It can be seen that more protoplasts transfected with *BnaNAC60* or *BnaNAC60ΔTM* plasmids were stained with Evans blue dye than *GFP* control protoplasts (Figure 3a). A quantitative comparison showed that death rates of protoplasts transfected with *BnaNAC60ΔTM* and *BnaNAC60* were over fourfold and threefold higher than that of the control, respectively (Figure 3c). Secondly, fluorescein diacetate (FDA) is a fluorescent dye for detecting living cells; only live cells stained with FDA can emit

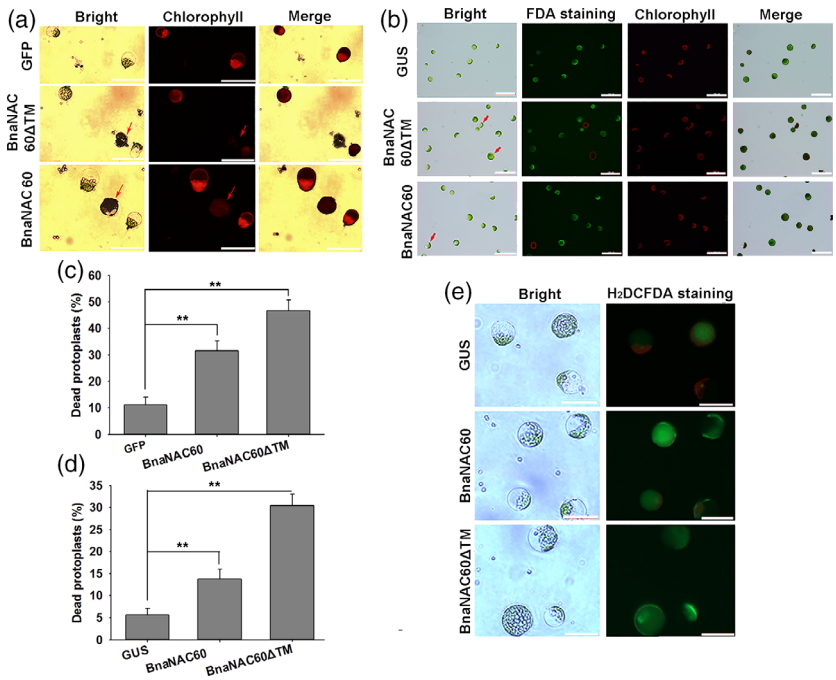

Figure 3. BnaNAC60 expression induced ROS accumulation and cell death in oilseed rape protoplasts. (a) Examination of cell death by Evans blue staining. Arrows represent dead protoplasts stained by Evans blue dye. Bars, 50 μm. (b) FDA staining to investigate the cell viability. Bars, 100 μm. Arrows indicate dead protoplasts. Autofluorescence of chloroplasts is shown in the second last panel in both (a) and (b). (c,d) Percentages of dead protoplasts as detected by Evans blue staining (a) and FDA staining (b). Data are presented as the mean of three replicates ± SE (n = 20). Asterisks indicate significant differences by Student's t-test (*$P \leq 0.05$; **$P \leq 0.01$). (e) Detection of ROS levels through the fluorescent H_2DCFDA dye. Green fluorescence indicates ROS. Bars, 50 μm.

fluorescence. FDA staining verified that 30.5% and 13.9% of protoplasts transfected with *BnaNAC60ΔTM* and *BnaNAC60* plasmids were dead, respectively; these percentages were significantly higher than that of the control (Figure 3b,d). In addition, a ROS-specific fluorescent dye, 2′,7′-dichlorodihydrofluorescein diacetate (H_2DCFDA), was used to detect the accumulation of ROS. We found that protoplasts transfected with *BnaNAC60ΔTM* and *BnaNAC60* plasmids showed stronger fluorescence than controls (Figure 3e). These results collectively demonstrated that BnaNAC60 positively modulates cell death and ROS accumulation in oilseed rape too.

BnaNAC60 binds to a *cis*-element sequence other than NACRS

Next, we aimed to identify the direct target genes of BnaNAC60 to better understand its function. One prerequisite is to identify the *cis*-element bound by BnaNAC60. Previous work on the recognition sites of representative ANAC TFs has identified a couple of sites for several NACs (Lindemose *et al.*, 2014). Specifically, members of the stress-responsive NAC (SNAC) subfamily were previously shown to bind to the consensus motif TTNCGT(G/A) (NAC recognition sequence, NACRS) in the promoters of target genes (Puranik *et al.*, 2012). It has also been reported that the putative binding element for NTL8/ANAC040 is TTNCTT (Lindemose *et al.*, 2014), which is named NTLBS in this study. A phylogenetic analysis of BnaNAC60 indicated it was clustered together with NTL8 (Figure S2). We therefore hypothesized that BnaNAC60 may be able to recognize and bind to this element too. To test this, we conducted a dual-luciferase (LUC) reporter assay. Five tandem repeats of TTNCTT sequences named 5xNTLBS were synthesized and inserted, together with the CaMV35S minimal promoter upstream of the firefly *LUC* gene (Figure 4a). The *Renilla luciferase* (*REN*) gene driven by the CaMV35S promoter was co-expressed as an internal control. Expression of the full-length *BnaNAC60* and the active *BnaNAC60ΔTM* was driven by the CaMV35S promoter and they were used as the effectors. GUS was used as the control. The results showed that BnaNAC60ΔTM, but not BnaNAC60, strongly activated the 5xNTLBS-35Smin controlled *LUC* expression with LUC/REN ratios significantly increased compared with the GUS control at two time points (Figure 4b). In contrast, neither BnaNAC60 nor BnaNAC60ΔTM significantly activated the expression of *LUC* when driven by the NACRS-35Smin promoter (Figure S17), suggesting that NACRS is not a *cis*-element recognized by BnaNAC60.

To confirm the binding of BnaNAC60 to NTLBS, an electrophoretic mobility shift assay (EMSA) was performed. For this purpose, the glutathione S-transferase (GST)-BnaNAC60ΔTM fusion protein was purified from *Escherichia coli*. An examination of the purity indicated it was

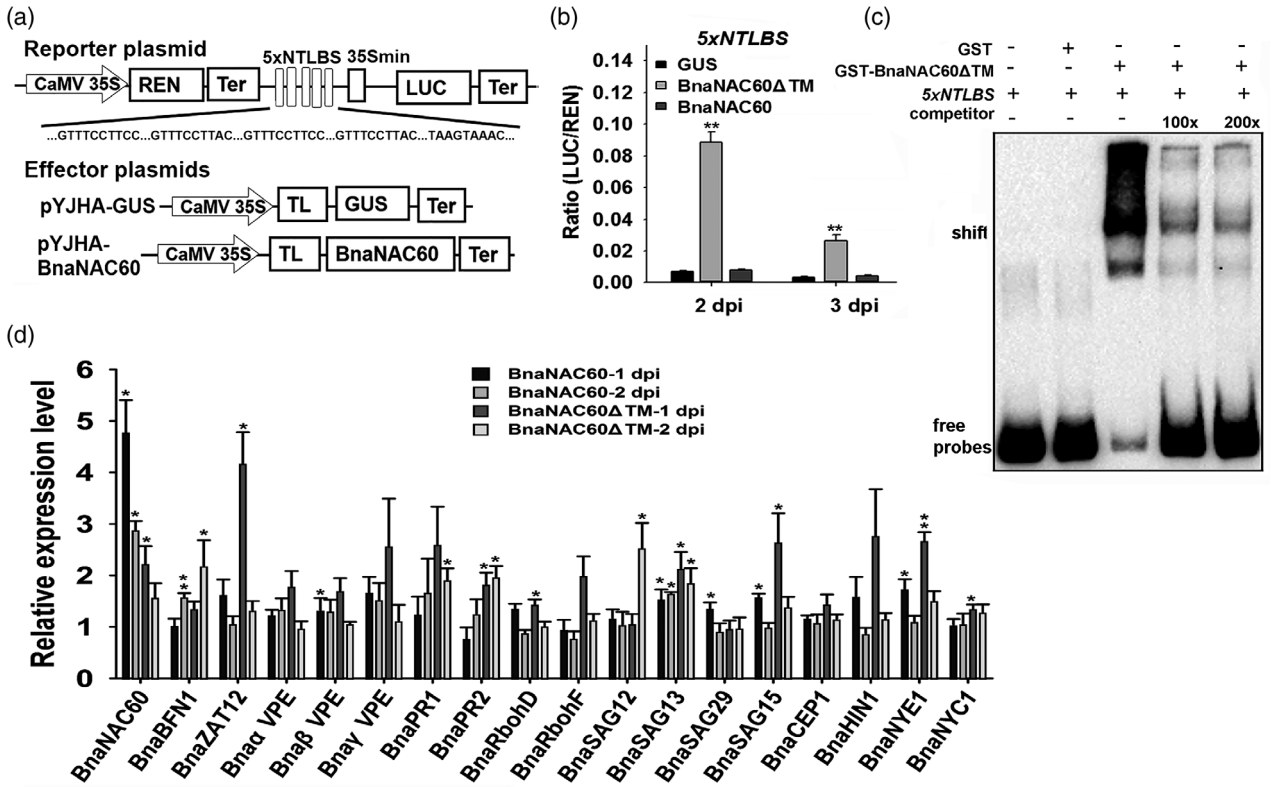

Figure 4. Identification of the binding motif of BnaNAC60 and expression analysis of marker genes. (a) A schematic diagram showing the double reporter and effector plasmids. The double reporter plasmid contains the synthetic 5xNTLBS elements fused to the minimal promoter sequence of CaMV35S inserted upstream of the *LUC* reporter gene. *Renilla luciferase* (*REN*) driven by the CaMV35S promoter included in the same construct served for internal normalization. The effector plasmid contains *BnaNAC60* or its truncated form *BnaNAC60ΔTM* driven by CaMV35S. A GUS expression plasmid was used as the control effector. TL, translational leader sequence; Ter, transcriptional termination sequence. (b) A dual-luciferase assay of BnaNAC60-mediated transactivation of the *LUC* reporter gene driven by 5xNTLBS-35S min promoter in *N. benthamiana* leaves. Ratios of LUC to REN activities were used to reflect the transcriptional ability. Asterisks indicate significant differences by Student's *t*-test (**$P \leq 0.01$). (c) Electrophoretic mobility shift assay (EMSA) of BnaNAC60ΔTM binding to the 5xNTLBS element labeled with biotin. The GST-BnaNAC60ΔTM fusion protein was used to detect its binding ability to 5xNTLBS and the GST protein was used as a negative control. Competitor (unlabeled probes) was used in molar excess. The bands in the upper and lower panels indicate shift (protein–DNA complex) and unbound free probes, respectively. (d) Transcript abundance analysis of ROS-, cell death-, senescence-, and defense- related marker genes in cotyledons of oilseed rape transiently expressing *BnaNAC60* and *BnaNAC60ΔTM*. Transcript levels were measured at two time points (1 and 2 dpi). *GFP*-expressing tissues were used as the control. Data represent the geometric mean ± SE of three biological replicates. The *BnaUP1* and *BnaUBC9*genes were used as the endogenous references. Asterisks indicate significant differences compared to*GFP*-expressing tissue by Student's *t*-test (*$P \leq 0.05$; **$P \leq 0.01$).

sufficient, and its molecular weight was as predicted (Figure S18). 5xNTLBS probes were labeled with biotin. GST alone was also expressed and purified independently to be used as a control. As shown in Figure 4(c), GST-BnaNAC60ΔTM bound to 5xNTLBS, forming a DNA–protein complex, which migrated more slowly than free probes. When unlabeled DNA fragments were added in excess, the signal intensity of the shifted band was strongly reduced. Collectively, these data indicate that BnaNAC60ΔTM binds to NTLBS directly and specifically.

BnaNAC60 modulates the expression of genes related to cell death, ROS, senescence, and defense

In order to explore the molecular mechanism underlying the function of BnaNAC60, we performed qRT-PCR to examine the expression of an array of marker genes involved in PCD, ROS accumulation, defense, and leaf senescence. To this end, *BnaNAC60* and *BnaNAC60ΔTM* were individually transiently expressed in 10-day-old oilseed rape seedlings, and the *GFP* gene was expressed as the control. The results showed that *BnaNAC60* expression was significantly induced at 1 and 2 dpi in seedlings overexpressing full-length *BnaNAC60*, while it was significantly induced only at 1 dpi in seedlings overexpressing *BnaNAC60ΔTM*. *BnaBFN1* expression was slightly induced at 1 dpi, but was significantly induced at 2 dpi (Figure 4d). *BnaZAT12* expression was significantly induced at 1 dpi and was mildly induced at 2 dpi in *BnaNAC60ΔTM*-overexpressing seedlings. Expression of *BnaβVPE* was significantly induced at 1 dpi, while *BnaαVPE* and *BnaγVPE* expression was induced at 1 dpi as well (Figure 4d). Besides, the expression levels of *BnaRbohD* and *BnaRbohF* were examined and both were induced at 1 dpi, with the change in *BnaRbohD* levels being significant in

BnaNAC60ΔTM-overexpressing seedlings (Figure 4d). SAG and Pathogenesis-Related (PR) genes are prominently induced during leaf senescence and HR, so the expression of these marker genes was also examined. The results showed *BnaSAG13* and *BnaSAG15* expression was significantly induced at one or two time points, and *BnaSAG12* expression was also induced at 2 dpi in *BnaNAC60ΔTM*-overexpressing seedlings; however, *BnaSAG29* expression was induced only at 1 dpi in *BnaNAC60*-overexpressing seedlings (Figure 4d). *BnaPR1* expression was significantly induced at 2 dpi, while *BnaPR2* expression was significantly induced at both time points in *BnaNAC60ΔTM*-overexpressing seedlings only. *BnaCEP1*, similar to *BnaSAG12*, encoding a papain-like cysteine protease involved in tapetal PCD and pollen development (Zhang *et al.*, 2014), was also detected but its expression showed no significant change (Figure 4d). *Harpin Inducing 1* (*HIN1*) or its Arabidopsis ortholog *Yellow Leaf-Specific 9* (*YLS9*), whose expression is highly induced during HR-like cell death and leaf senescence (Zheng *et al.*, 2004), was also analyzed. The result showed that *BnaHIN1* was induced at 1 dpi only (Figure 4d). In addition, we examined two chlorophyll degradation genes (*NYC1* and *NYE1*), and the data showed that both *BnaNYC1* and *BnaNYE1* were significantly induced at 1 dpi only (Figure 4d). Overall, the magnitude of increase in transcript levels in *BnaNAC60*-overexpressing seedlings was much lower than that in *BnaNAC60ΔTM*-overexpressing seedlings.

To further examine the expression changes of these genes, we performed a similar assay using oilseed rape protoplasts. A Western blot assay confirmed the expression of *BnaNAC60ΔTM*, *BnaNAC60*, and *GFP* (control) in protoplasts (Figure S19a). The results showed that the expression of *BnaBFN1*, *BnaαVPE*, *BnaβVPE*, *BnaγVPE*, *BnaRbohD*, *BnaSAG13*, *BnaSAG15*, and *BnaNYC1* was significantly induced in the *BnaNAC60ΔTM*-overexpressing protoplasts, while transcripts of these genes did not show any significant change in *BnaNAC60*-overexpressing protoplasts (Figure S19b). These results suggested that BnaNAC60 mediates ROS accumulation and cell death likely through inducing the expression of some of these key genes.

Given that transient expression of *BnaNAC60* in *N. benthamiana* leaves also caused severe cell death and ROS accumulation (Figure S8), we also examined the changes in transcript abundance of representative marker genes in tobacco to confirm the similarity of BnaNAC60 function in different expression systems. Most of these marker genes showed significant changes in the *BnaNAC60ΔTM*-overexpressing tissues; however, no significant change or much smaller changes were observed in *BnaNAC60*-overexpressing tissues. The expression of *NbRbohB* (ortholog of *RbohD* in Arabidopsis and oilseed rape) was slightly induced at 3 dpi (Figure S20a) and the expression of *NbRbohA* (ortholog of *RbohF*) did not show any significant change as a result of *BnaNAC60ΔTM* expression. *NbVPE3* expression was significantly induced at 3 dpi among the four VPE genes examined here. Similarly, none of the three metacaspase genes showed any difference. The expression of *Zinnia Endonuclease 1* (*ZEN1*), which is the homolog of *BFN1* in Arabidopsis involved in PCD of apical bud meristem (Aoyagi *et al.*, 1998), was highly induced in *BnaNAC60ΔTM*-overexpressing tissues, with a fold change of 38 and 42 at 2 and 3 dpi, respectively (Figure S20a). Moreover, the expression of *NbSAG12* and *NbSAG101* was also identified to be significantly induced at 2 dpi, and the latter encodes an acyl hydrolase involved in senescence (He and Gan, 2002). *NbZAT12* expression was highly induced at 3 dpi as well (Figure S20b). The expression of *NbLDS1* and *NbLOL1*, encoding two antagonistic regulators of cell death and defense (Epple *et al.*, 2003), was induced and repressed, respectively. Lastly, the expression of the defense response marker genes *NbPR2*, *NbPR5*, *NbHIN1*, *NbACRE31,* and *NbCYP71D20*, which is induced in HR-like cell death or by pathogen attack (Pontier *et al.*, 1999), was mostly induced by BnaNAC60ΔTM as well (Figure S20b).

BnaNAC60 positively modulates the promoter activities of genes involved in ROS production, PCD, and leaf senescence

The above investigations indicated that some of these induced genes may constitute the regulon of BnaNAC60 and part of them may be direct targets. We therefore performed a LUC reporter assay to examine the ability of BnaNAC60 and its active form BnaNAC60ΔTM to activate the transcription of these genes. Promoter regions (including 5′ UTRs) of these marker genes were fused upstream of the *LUC* gene, which was used as a reporter. The *REN* gene driven by the CaMV35S promoter was used as the internal control (Figure 5a). The plasmids expressing BnaNAC60ΔTM or BnaNAC60 and GUS (control) were used as effectors. LUC/REN ratios reflected the ability of BnaNAC60 to transcriptionally activate its putative downstream genes. The results showed that co-expression of *BnaNAC60* or *BnaNAC60ΔTM* with *ProBnaZAT12:LUC* and *ProBnaBFN1:LUC* significantly increased LUC/REN ratios at 2 and 3 dpi (Figure 5b,h). In addition, LUC/REN ratios of *ProBnaRbohD, ProBnaγVPE,* and *ProBnaNYE1* reporters increased about twofold at 3 dpi when *BnaNAC60ΔTM* was used as the effector (Figure 5c,f,g). Besides, BnaNAC60ΔTM significantly induced the expression of *LUC* driven by promoters of *ProBnaαVPE*, *ProBnaβVPE,* and *ProBnaNYC1* compared with the GUS control at the two time points (Figure 5d,e,i). In contrast, neither BnaNAC60 nor BnaNAC60ΔTM increased the activities of *ProBnaδVPE* and *ProBnaRbohF* (Figure S21), suggesting these two genes are not regulated directly by BnaNAC60.

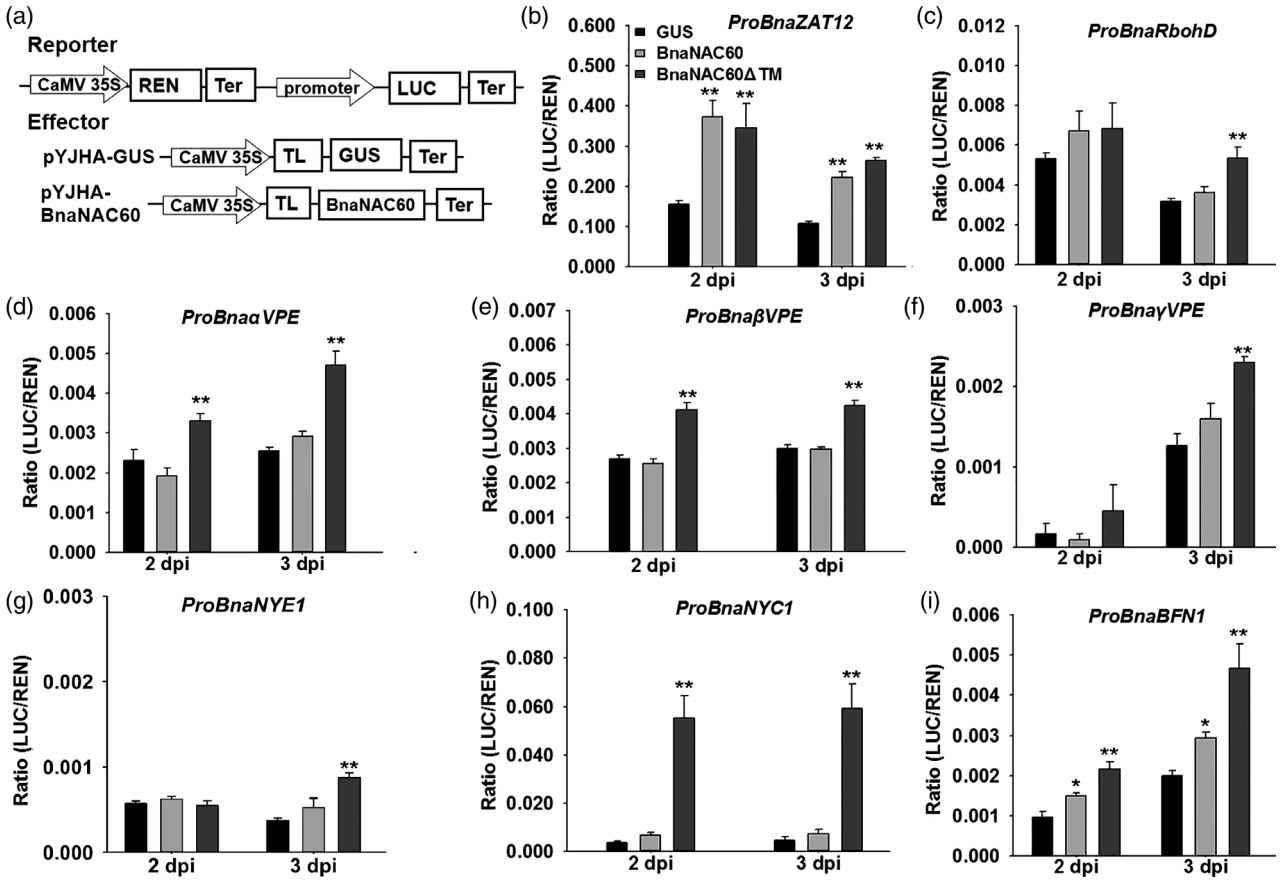

Figure 5. The dual-luciferase reporter assay of transcriptional activation of putative target genes by BnaNAC60. (a) A schematic diagram of the double reporter and effector plasmids. LUC and REN represent firefly luciferase and *Renilla* luciferase, respectively. pYJHA-GUS plasmid was used the control effector. Ter, terminatior sequence of transcription. (b–i) Examination of the ability of BnaNAC60 and BnaNAC60ΔTM to activate the transcription of the *LUC* reporter gene under the control of different promoter regions of marker genes from oilseed rape. Relative reporter activity was normalized by the ratio of LUC/REN. Data were from three independent replicates ± SE at two time points. dpi, days post-infiltration. Asterisks indicate significant differences compared to the GUS effector by Student's *t*-test (*$P \leq 0.05$; **$P \leq 0.01$).

BnaNAC60 binds to promoters of target genes both *in vitro* and *in vivo* through the NTLBS *cis*-element

To explore whether there was a direct regulatory relationship between BnaNAC60 and the aforementioned putative target genes, we analyzed the promoter regions of *BnaRbohD*, *BnaαVPE*, *BnaβVPE*, *BnaγVPE*, *BnaNYC1*, *BnaZAT12,* and *BnaBFN1*. It was revealed that multiple NTLBS elements (5′TT(N)CTT3′ or 5′AAG(N)AA3′) were present in the promoters of these genes (Figure 6a). Next, EMSA was performed to determine the binding *in vitro*. The results showed that BnaNAC60ΔTM bound to the F2, F3, and F4 segments of the *BnaRbohD* promoter, but not to F1. As for the three *VPE* promoters, BnaNAC60ΔTM bound to the F1, F2, and F4 segments of *ProBnaαVPE*, the F2 and F3 segments of *ProBnaβVPE*, and the F1 and F2 segments of *ProBnaγVPE*, and no binding was detected with the other labeled probes (Figure 6b). Besides, BnaNAC60ΔTM bound to four probes of *ProBnaNYC1* except its F5 segment. Moreover, BnaNAC60ΔTM bound to the F1 and F2 segments of the *BnaBFN1* promoter, but not to the F3 segment (Figure 6b). Lastly, only the F3 segment of *ProBnaZAT12* was bound by BnaNAC60ΔTM (Figure 6b). As a control, purified GST protein alone did not bind to any of these labeled segments. To further confirm the binding specificity, a competition assay was performed. The results showed that when the unlabeled probes were added in excess, the binding shifts became weaker or even disappeared (Figure S22), supporting the conclusion that BnaNAC60ΔTM binds specifically to the respective fragments of putative target genes *in vitro*.

To further examine whether these genes are direct targets of BnaNAC60 *in vivo*, chromatin immunoprecipitation (ChIP)-qPCR was performed. An antibody specific to the HA epitope tag was used to collect chromatin DNA bound by BnaNAC60ΔTM. The utility and specificity of the anti-HA antibody was examined and good results were obtained (Figure S23a). Agarose gel electrophoresis was also

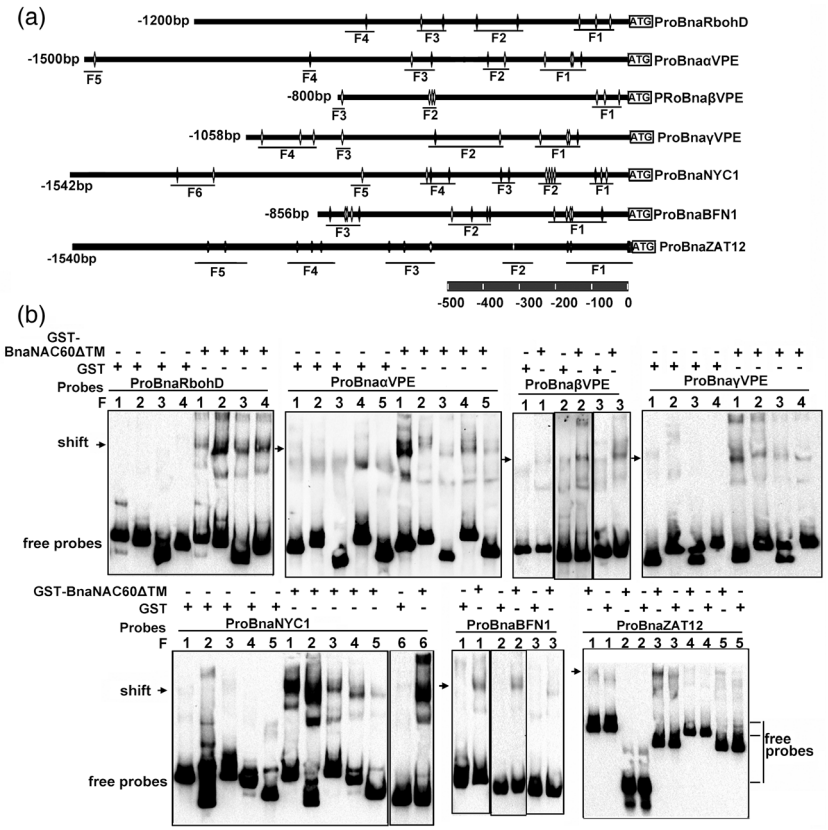

Figure 6. Electrophoretic mobility shift assay (EMSA) of BnaNAC60ΔTM binding to different fragments in the promoter regions of putative target genes. (a) Schematic diagrams of NTLBS elements in the promoters of putative target genes. White and black diamonds indicate the binding elements on sense and antisense strands, respectively. The promoter lengths and sites of NTLBS elements are drawn in scale. Fxs represent the fragments tested by EMSA. ATG is the translational start codon. (b) Assay of GST-BnaNAC60ΔTM fusion protein binding to different biotin-labeled fragments of promoter regions of putative target genes. GST protein was used as a negative control. Competitor probes (unlabeled) were added in molar excess as shown above the images. '+' and '−' represent the presence and absence of one component in binding reactions, respectively. Shifts indicate the protein–DNA complex while free probes mean unbound probes.

performed to ensure the quality of chromatin DNA fragments after sonication. As shown in Figure S23(b), the size of the DNA smear was mostly located between 200 bp and 1 kb, indicating a good quality. Immunoprecipitated chromatin DNA was thus subjected to qPCR analysis. Primers were designed according to the previous EMSA results, and were subjected to PCR amplification and agarose gel electrophoresis examination before use. Primers that did not show good specificity were discarded and designed again before further testing. As a negative control, primers targeting a region located at least 1 kb far from the binding site were designed, tested, and used in parallel (Figure 7a). Our results showed that BnaNAC60ΔTM significantly enriched the P1–P3 fragments of the *BnaRbohD* and *BnaαVPE* promoters, the P1 and P2 fragments of the *BnaβVPE*, *BnaγVPE,* and *BnaBFN1* promoters, the P1 fragment of the *BnaZAT12* promoter, and the P1–P5 fragments of the *BnaNYC1* promoter (Figure 7b). In contrast, no significant enrichment of control fragments (CK) was detected for any of these seven genes. Collectively, these results indicate that the active form of BnaNAC60 binds to the promoter of ROS production-, PCD-, and leaf senescence-related genes via the consensus NTLBS sequence.

DISCUSSION

Leaf senescence is a highly coordinated process influenced by the massive reprogramming of gene expression through the action of TFs (Kim *et al.*, 2016). Investigation and illumination of the mechanisms modulating plant senescence have great potential for improving crop yield, stress tolerance, and nutritional quality (Uauy *et al.*, 2006; Rivero *et al.*, 2007). NAC TFs are plant-specific and play diverse roles in plant development, abiotic and biotic stress responses, and leaf senescence (Olsen *et al.*, 2005; Puranik *et al.*, 2012). A few members of the NAC family have been reported to positively or negatively modulate leaf senescence in Arabidopsis, rice, tomato, wheat and cabbage (*Brassica rapa*) (Guo and Gan, 2006; Balazadeh *et al.*, 2010, 2011; Wu *et al.*, 2012; Kim *et al.*, 2013; Liang *et al.*, 2014; Mahmood *et al.*, 2016; Oda-Yamamizo *et al.*,

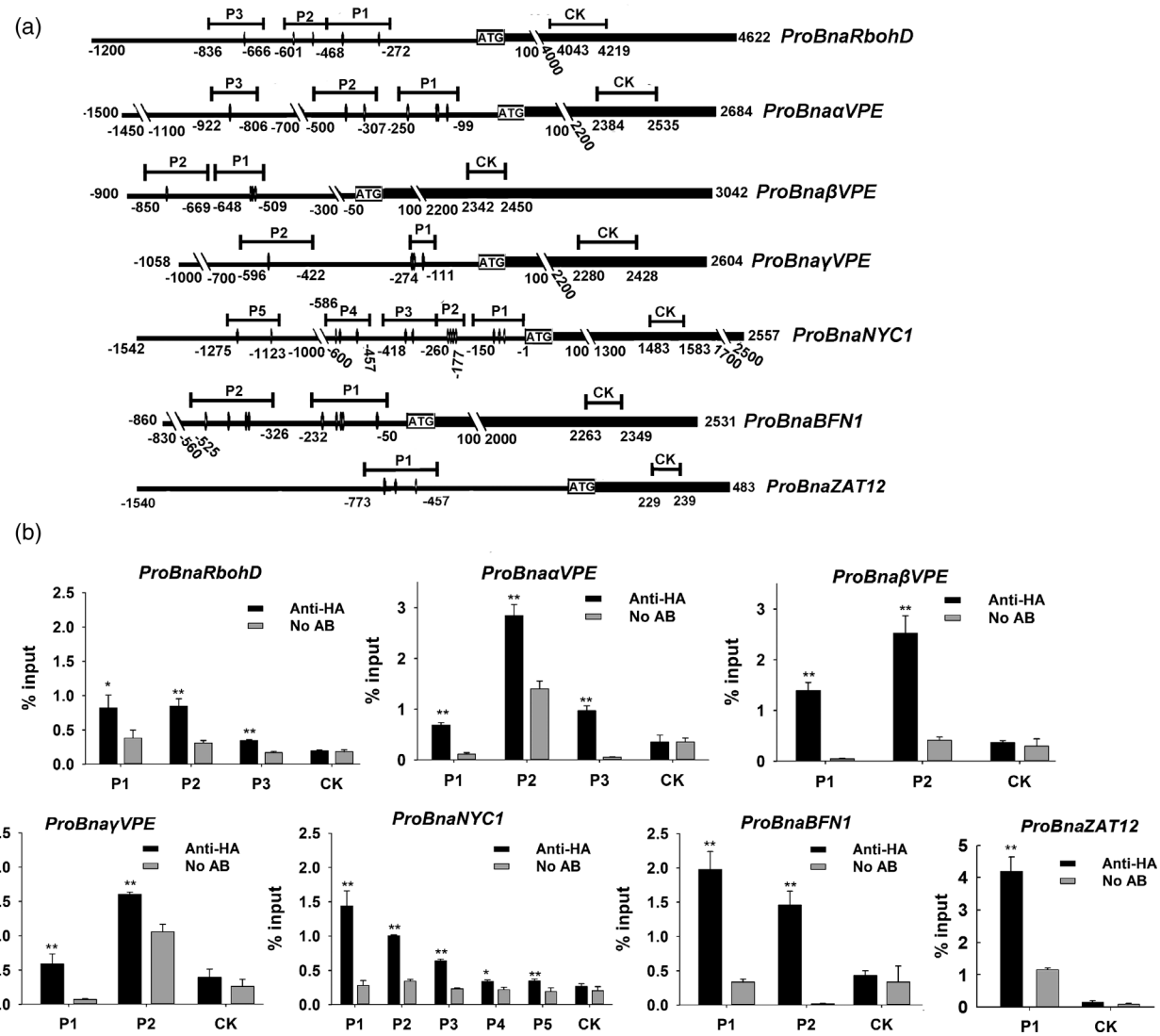

Figure 7. ChIP-qPCR assay of binding of BnaNAC60ΔTM to the promoter regions of target genes in oilseed rape. (a) Schematic representation of NTLBS elements in promoter regions of target genes. ATG, translational start codon. The diamonds indicate the NTLBS binding elements. The thin black bars indicated by Pxs above the promoters represent regions which were amplified in qPCR and the numbers show the distance (in bp) from the ATG start codon. CK, genomic control regions amplified in qPCR in parallel. (b) ChIP-qPCR results. Chromatin DNA was co-immunoprecipitated with anti-HA antibody or no antibody. Fragmented genomic DNA was released from the protein–DNA complexes and subjected to qPCR analysis. Input sample was used to normalize the qPCR results in each ChIP sample. Data are presented as the mean ± SE of three biological replicates. Asterisks indicate significant differences by Student's *t*-test (*$P \leq 0.05$; **$P \leq 0.01$).

2016; Pimenta *et al.*, 2016; Mao *et al.*, 2017; Fan *et al.*, 2018; Ma *et al.*, 2018). Despite the importance of understanding how developmental and environmental signals are integrated to modulate leaf senescence in oilseed rape, the transcriptional control of leaf senescence in this important crop plant remains poorly understood.

In this study, we demonstrated that a membrane-tethered NAC60 in oilseed rape is involved in age-dependent leaf senescence and may integrate stress signals, ROS signaling, and PCD with an inner natural leaf senescence program through activating different but related target genes. BnaNAC60 is associated with the ER and its expression can be induced by ER and oxidative stresses to translocate to nuclei (Figure 1b; Figures S5 and S7). In this aspect, BnaNAC60 is very different from its ortholog in Arabidopsis Col-0, which has no transmembrane domain at all and is targeted to nuclei only (Figure S3) (Liang *et al.*, 2015). BnaNAC60 is phylogenetically close to ANAC089 (Figure S2), an NTL previously reported to modulate ER stress-induced PCD in Arabidopsis (Yang *et al.*, 2014b). Consistently, BnaNAC60 showed an ability to activate the expression of several unfolded protein response marker genes under ER stress conditions (Figure S6), which is, to some degree, different from ANAC089 (Yang *et al.*, 2014b).

Moreover, transient heterologous expression of *ANAC060* from Arabidopsis Col-0 in tobacco leaves indicated that ANAC060, unlike BnaNAC60, failed to induce ROS accumulation or HR-like cell death (Figure S10). A previous report indicated ANAC060 from ecotype C24 is different from that in ecotype Col-0 in that ANAC060 from C24 is an NTL, and this shorter version of the ANAC060 protein is found in approximately 12% of natural Arabidopsis accessions (Li *et al.*, 2014). A quantitative comparison of identities indicates that BnaNAC60 is more similar to ANAC060 (C24, with an identity of 87.5%) than to ANAC060 (Col-0, 84.2% identity). However, different from BnaNAC60, ectopic overexpression of neither *ANAC060* nor *ANAC060ΔTM* from C24 induced any significant cell death or ROS accumulation (Figure S11). These results suggest that the function of ANAC060 is different from that of BnaNAC60, at least in terms of ROS, PCD, and leaf senescence, though ANAC060 from C24 is more similar to BnaNAC60, at least in amino acid sequence. An examination of the domain of ANAC060 from Col-0 suggests that it is likely still functional as it contains the typical domains of a regular NAC TF, including an N-terminal NAC domain harboring five subdomains (A, B, C, D, E) and a C-terminal transcriptional regulatory domain (Figure S1).

NTLs are usually inactive or in a dormant state through association with the cellular membrane system via their transmembrane domains (Kim *et al.*, 2010a). Upon internal and environmental stimuli, NTLs could be activated through proteolytic cleavage either by membrane-associated proteases or by the ubiquitination-dependent proteasome (Kim *et al.*, 2010a). This constitutes an intriguing mechanism of ensuring rapid transcriptional responses to internal and environmental changes as transcriptional and translational regulations are skipped (Chen *et al.*, 2008; Seo *et al.*, 2008). Although the mechanisms of a few NTLs in Arabidopsis entering nuclei have been explored (Seo *et al.*, 2010; Kim *et al.*, 2010a), for instance, ANAC017 may be cleaved by a rhomboid protease (Ng *et al.*, 2013), there is no uniform pathway for all NTLs. Previous studies have shown that increased levels of endogenous ROS induced by various environmental stresses such as drought, salt, and extreme temperatures as well as some developmental changes can induce leaf senescence and cell death (Khanna-Chopra, 2012; Lee *et al.*, 2012; Woo *et al.*, 2013). Accumulation of ROS can cause protein and lipid dysfunction as well as chlorophyll degradation, which are typical syndromes accompanied with leaf senescence (Lim *et al.*, 2007). We found that Tn and H_2O_2 treatments triggered the membrane release of BnaNAC60 (Figures S5 and S7), indicating that the activity of BnaNAC60 is mediated by controllable membrane release and follow-up nuclear localization, which ensures rapid adaptation responses to environmental changes and the progression of leaf senescence. Stress-induced activation of membrane-tethered NAC proteins have been reported with NTL4 (ANAC053), NTL6 (ANAC062), and NTL17 (ANAC089) in Arabidopsis (Seo *et al.*, 2010; Lee *et al.*, 2012; Yang *et al.*, 2014a,b).

The expression of *BnaNAC60* was induced during leaf senescence (Figure 1c), suggesting that the function of it may be linked to the age-dependent leaf senescence program. *BnaNAC60* expression was also induced by a set of environmental stresses and phytohormones, including drought, salt, ABA, and MV (Figure 1d), which are generally positively involved in leaf senescence. To substantiate the role of BnaNAC60, we provided several lines of evidences to support that it plays a positive role in natural leaf senescence. Initially, we demonstrated that constitutive overexpression of the activated form of *BnaNAC60* (i.e., *BnaNAC60ΔTM*) accelerates leaf senescence, which was reflected in quite a few hallmarks such as leaf yellowing, H_2O_2 accumulation, chlorophyll degradation, ion leakage, and increased expression of senescence- and PCD-associated marker genes (Figure 2; Figure S13). We further showed that transient expression of *BnaNAC60* in leaves of tobacco also led to a similar phenotype, with the phenotype of *BnaNAC60* being much weaker than that of *BnaNAC60ΔTM*, as indicated by the measurements of relevant physiological indices (Figure S8). The function of *BnaNAC60* in protoplasts of oilseed rape was also tested and showed expected results (Figure 3), which is highly similar to rice *NAC4* (Kaneda *et al.*, 2009). Different from SNAC-type NAC TFs, BnaNAC60 showed great affinity towards the NTLBS element (Figure 4), but not towards the NACRS element (Figure S17). Furthermore, screening of a collection of marker genes related to ROS, PCD, defense responses, and leaf senescence via qRT-PCR and dual-LUC reporter techniques revealed that BnaNAC60 may modulate the transcription of multiple genes from this collection (Figures 2e, 4d, 5; Figures S19 and S20). We also observed that *ProBnaZAT12:LUC* and *ProBnaBFN1:LUC* were activated by both BnaNAC60 and BnaNAC60ΔTM, which suggests the regulatory effect of BnaNAC60 and BnaNAC60ΔTM on different promoters is different, as a basal level of proteolytically processed, activated BnaNAC60 proteins is expected to exist in cells. Through *in vitro* EMSA and *in vivo* ChIP-qPCR techniques, we showed that the active form of BnaNAC60 bound directly to the promoter regions of *BnaRbohD*, *BnaαVPE*, *BnaβVPE*, *BnaγVPE*, *BnaNYC1*, *BnaBFN1,* and *BnaZAT12* (Figures 6 and 7; Figure S22). Thus, this study has built a direct link between BnaNAC60 function and genes whose encoded proteins participate in ROS production, PCD, and chlorophyll degradation.

Among the target genes, *RbohD* is responsible for ROS production in many processes, including pathogen infection (Torres *et al.*, 2002). As ROS levels have to be tightly restrained to avoid detrimental consequences to plant cells, RbohD is not only modulated by post-translational

phosphorylation but is also under transcriptional control by TFs (Kadota *et al.*, 2015). Previously, it was reported that *RbohC* and *RbohE* are regulated by transmembrane motif 1-like 4 (NTL4, also referred to as ANAC053) to mediate drought-induced leaf senescence (Lee *et al.*, 2012). This indicates that different NTLs may target different members of the RBOH gene family. ZAT12 is a member of the C2H2-type plant-specific zinc finger TF family and its expression is induced by many different types of abiotic stresses, including oxidative stress; ZAT12 is also required for the upregulation of many ROS signaling genes (Rizhsky *et al.*, 2004; Davletova *et al.*, 2005). Here, we identified *BnaZAT12* as a direct target of BnaNAC60 and we found that the expression of *BnaZAT12* is induced by BnaNAC60.

Interestingly, we also found that BnaNAC60 targeted multiple VPE genes, indicative of the execution of a cell death program. VPEs are cysteine proteases exhibiting caspase-like activity (Hara-Nishimura *et al.*, 2005). Originally found to be responsible for the maturation of seed storage proteins and vacuolar proteins, VPEs have also been shown to trigger vacuolar collapse-mediated PCD during defense responses and development (Hatsugai *et al.*, 2004). Here, we reported that overexpression of the activated form of *BnaNAC60* led to premature leaf senescence, cell death, and upregulation of *VPEs* (Figure 4; Figure S19), suggesting activation of VPEs and dPCD play a role in this process. De-greening of leaves as a consequence of chlorophyll degradation is a characteristic of leaf senescence (Hortensteiner and Krautler, 2011). NYC1 is a Chl b reductase catalyzing the first step of Chl degradation (Horie *et al.*, 2009). Overexpression of *BnaNAC60ΔTM* promoted *NYC1* expression and trans-activated its promoter (Figures 2e, 4d, 5h; Figure S19). Recent studies demonstrated that ANAC019/055/072 can directly promote the expression of three *CCGs* (*NYE1*, *NYE2,* and *NYC1*) in jasmonate (JA)-triggered Chl degradation (Zhu *et al.*, 2015); ORE1 (ANAC092) also activates the expression of *CCGs* in ethylene-triggered Chl degradation (Qiu *et al.*, 2015); ANAC016 can directly induce *NYE1* transcription (Sakuraba *et al.*, 2016); and ANAC046 positively modulates the expression of *CCGs* and leaf senescence (Oda-Yamamizo *et al.*, 2016). These data suggest that distinct NACs could be recruited individually or together to ensure a temporally and spatially coordinated regulation of Chl degradation leading to leaf senescence through different signaling pathways in different scenarios.

BFN1 is among the genes that are positively regulated by BnaNAC60 (Figures 2e, 4d, 5i; Figure S19). It encodes a type I nuclease responsible for the degradation of RNA and single-stranded DNA during several growth and developmental processes, sharing high similarity to *ZEN1*, which is associated with PCD in *Zinnia elegans* (Ito and Fukuda, 2002). *BFN1* expression was found to be specifically increased during leaf and stem senescence (Perez-Amador *et al.*, 2000). In addition, *BFN1* is also specifically expressed in the leaf and fruit abscission zones, suggesting an involvement in dPCD (Farage-Barhom *et al.*, 2008). In plants, age-induced dPCD occurs in all cell types of organs or even whole plants as the endpoint of plant senescence (Daneva *et al.*, 2016). Previously, ORE1 was found to target *BFN1* to modulate leaf senescence in Arabidopsis (Matallana-Ramirez *et al.*, 2013). However, the binding site of ORE1 is obviously different from that of BnaNAC60 (Figures 6 and 7), suggesting *BFN1* could be regulated by distinct NAC TFs as well.

In conclusion, this study has revealed an ER membrane-tethered NAC TF from oilseed rape, NAC60, that acts as an upstream regulator of ROS accumulation, cell death, and leaf senescence, likely through activating the expression of ROS-generating RbohD, the ROS signaling gene *ZAT12*, dPCD-associated *VPEs* and *BFN1*, and Chl degradation-related *NYC1* genes (Figure S24).

EXPERIMENTAL PROCEDURES

Plant materials and growth conditions

Seeds of oilseed rape (*B. napus*), tobacco (*N. benthamiana*), and Arabidopsis (ecotypes Col-0 and C24) were surface-sterilized for 1 min in 70% ethanol and then in 2.6% bleach solution (containing 0.01% Tween-20) for 2–4 min, before being washed four or five times in sterile deionized water. The seeds were stratified for 2 days at 4°C and germinated on 1/2 MS (Murashige and Skoog) medium (Caisson labs, USA, https://www.caissonlabs.com/) at 22°C in a greenhouse with a 14 h light/10 h dark photoperiod. Seven-day-old seedlings were transplanted to soil or used in other experiments.

Stress treatments and quantitative RT-PCR

Seven-day-old oilseed rape seedlings were transferred onto 1/2 MS medium supplemented with different hormones or other chemicals with normal 1/2 MS medium used as the control. For the cold and heat treatments, seedling plates were placed at 4°C and 38°C, respectively. Leaf tissues at different developmental stages were harvested at specific time points (Yan *et al.*, 2018). The whole process was repeated three times independently to prepare three biological replicates. Total RNA was extracted using a plant RNA kit (Omega Bio-tek, USA, https://www.omegabiotek.com/) and was treated with DNaseI (Ambion, USA, https://www.thermofisher.com/). cDNA synthesis was performed using 5 μg total RNA and RNaseH- M-MLV (Takara, Japan, https://www.takarabiomed.com.cn/). qRT-PCR was performed using SYBR GreenI premix (CWbio, China, https://www.cwbiotech.com/) on the CFX96 real-time system (Bio-Rad, USA, https://www.bio-rad.com/) with the following program: 10 min at 95°C, followed by 35 cycles of 95°C for 15 sec and 60°C for 1 min. Gene-specific primers were designed using PrimerSelect or Primer 3. The specificity and amplification efficiency were examined by BLAST and melting curve analyses. The reference genes used were *BnaUP1* and *BnaUBC9* for oilseed rape (Chen *et al.*, 2010) and *AtUBC21* and *AtUBQ10* for Arabidopsis (Czechowski *et al.*, 2005). Relative expression levels (fold changes) were calculated according to a previous formula (Pfaffl, 2001).

Subcellular localization assay

The coding sequences (CDSs) of *BnaNAC60* (full-length) and *BnaNAC60ΔTM* (deleted transmembrane domain) were amplified and fused downstream of *GFP* in the p35SNGFP binary vector, which was modified from pCsGFPBT (GenBank Accession No. DQ370426). *Agrobacterium tumefaciens* GV3101 cells were transformed with these constructs through a freeze-thaw method. Leaves of 28-day-old *N. benthamiana* were infiltrated and the GFP signals were detected after 2 days on a confocal microscope (Olympus, Japan, https://www.olympus-global.com/). The HDEL-mCherry marker (CD3-959) was described previously (Nelson *et al.*, 2007).

Plant transformation and leaf senescence assay

The CDSs of *BnaNAC60* and *BnaNAC60ΔTM* were subcloned into pHFGFP and pYJGFP binary vectors, respectively, which were modified from pCsGFPBT. Recombinant plasmids were introduced into *A. tumefaciens* GV3101, which was then used to transform wild-type *A. thaliana* (Col-0) plants via the floral dip method (Clough and Bent, 1998). Putative transformants (T1) were selected by placing seeds on agar-solidified 1/2 MS medium containing 25 mg L^{-1} hygromycin B (Amresco, USA, https://www.amresco-inc.com/). At the T3 generation, high-expression lines were screened through qRT-PCR. An empty vector pYJGFP carrying *GFP* alone was also transformed into wild-type *A. thaliana* plants separately. Seeds of homozygous T3 and control plants grown at the same time under identical standard conditions were used for the phenotypic assay (Yang *et al.*, 2018).

Isolation of protoplasts from oilseed rape and transient expression

The expression cassettes (CaMV35S::gene of interest followed by a terminator sequence) of individual genes were released from the above recombinant plasmids for overexpression through restriction before ligation into the pUC19 plasmid. Mesophyll cell protoplasts were isolated from the fifth and sixth leaves of 6-week-old oilseed rape plants grown under 14 h light/10 h dark conditions as previously described (Yoo *et al.*, 2007). Plasmid DNA (20 μg) was transfected into 2×10^5 protoplasts by a PEG4000/$CaCl_2$-mediated method. Transfected protoplasts were incubated at room temperature in 24-well plates for 14–16 h.

For the membrane-to-nucleus translocation analysis, Tn (Sigma-Aldrich, USA, https://www.sigmaaldrich.com/) was added to transfected protoplasts at a final concentration of 5 μg ml^{-1}, and cells were incubated for 6 h. For the H_2O_2 treatment, transfected protoplasts were subjected to 10 mM H_2O_2 (Alfa Aesar, France, https://www.alfa.com/) for 15 min and washed once with 1× PBS buffer, before incubation for a further 5 h. Images were taken on a laser confocal microscope (TCS-SP8, Leica, Germany, https://en.leica-camera.com/). For the staining, transfected protoplasts were incubated in a 0.05% Evans blue (MP Biomedicals, USA, https://www.mpbio.com/) staining buffer for 15 min or in a 0.01% FDA (MP Biomedicals) staining buffer for 5 min. After washing, images were taken on a fluorescence microscope (DM500B, Leica). Scoring of dead protoplasts was performed by counting 20 individual fields of three replicates. H_2DCFDA staining was performed as described previously (Yan *et al.*, 2018).

Measurement of hydrogen peroxide and DAB staining

About 0.1 g of fresh sample was extracted with 1 ml 5% (w/v) trichloroacetic acid (Alfa Aesar) buffer. After spinning, the supernatant was neutralized to pH 7.5 with 1 M NH_4OH (Alfa Aesar). Extract was divided into two aliquots of 100 μl. One aliquot supplemented with catalase (Sigma-Aldrich) was used as the control, and the other aliquot was processed without catalase. Both aliquots were supplemented with 400 μl of 0.1 M Tris-HCl followed by the addition of 500 μl colorimetric reagent. The colorimetric reagent was prepared freshly by mixing 1:1 (v/v) 0.3 mM potassium titanium oxalate (Alfa Aesar) and 0.3 mM resorcinol monosodium salt (Alfa Aesar). Absorbance at 508 nm was measured against a standard curve of H_2O_2, after incubation at room temperature for 15 min (Patterson *et al.*, 1984). For DAB (MP Biomedicals) staining, the detached leaves were incubated in DAB staining solution for 4 h at room temperature and decolorized in a destaining solution at 95°C for 15 min (Sun *et al.*, 2014).

Chlorophyll, anthocyanin, and malonaldehyde content measurements and electrolyte leakage assay

Chlorophyll, anthocyanin, and MDA contents were quantified as described previously (Chen *et al.*, 2016). For the electrolyte leakage assay, about 0.1 g of leaf tissue was immersed in 5 ml of deionized water. After applying vacuum for 15 min and shaking at 180 rpm for 1 h at 25°C, the electrical conductivity of samples (C1) and deionized water (C0) was determined with an electrical conductivity meter (Leici, China, http://www.lei-ci.com/). Samples were boiled for 15 min and allowed to cool to room temperature, and the electrical conductivity of samples (C2) and deionized water (C0′) was determined again. Total relative ion leakage was calculated as follows: relative ion leakage (%) = $((C1 - C0) / (C2 - C0')) \times 100\%$.

Dual-luciferase reporter assay

The CDSs of *BnaNAC60* and *BnaNAC60ΔTM* were amplified and inserted into the binary pYJHA vector (modified from pCsGFPBT) and used as effectors. The GUS-encoding gene cloned into the same empty vector, resulting in pYJHA-GUS, was used as the control effector. Promoters plus 5′ UTRs were amplified from genomic DNA using PCR mediated by high-fidelity PrimeSTAR HS DNA polymerase (TaKaRa, Japan). The promoters were inserted into vector pGreenII0800-LUC (Hellens *et al.*, 2005), in which *REN* driven by the 35S promoter was used as the endogenous control. *Agrobacterium* cultivation and infiltration into *N. benthamiana* leaves were performed as described previously (Yan *et al.*, 2018). Leaf discs were harvested at 2 and 3 dpi. Samples were ground in liquid nitrogen with luciferase activities measured using a Dual-Luciferase Reporter Assay kit (Promega, USA, https://www.promega.com/).

Protein purification and electrophoretic mobility shift assay (EMSA)

The CDS of *BnaNAC60ΔTM* was recombined into the pGEX 4T-1 vector, and transformed into *E. coli* strain Rosetta (DE 3) (Novagen, Germany, http://www.merckmillipore.com). Fusion protein expression was induced at 25°C by 0.1 mM isopropyl β-D-thiogalactoside (Amresco) for 8 h. Cells were harvested by centrifugation at 12 000 ***g*** for 20 min and lysed by ultrasonication. The supernatant was used for protein purification via GST bind resin (Merck, Germany, http://www.merckmillipore.com). Double-stranded probes were either annealed from synthesized single-stranded primers (Sangon, China, https://www.sangon.com/) or amplified by the high-fidelity *Pfu* polymerase (Bioer, China, http://www.bioer.com.cn/). Primers are listed in Table S1. EMSA was performed using a LightShift chemiluminescent EMSA kit (Thermo Scientific, USA, https://www.thermofisher.com/). After binding reactions, samples

were loaded into a 5% non-denatured polyacrylamide gel and blotted onto a positively charged nylon membrane (GE Healthcare, USA, https://www.gehealthcare.com/) under UV cross-linking. Signals were detected using the streptavidin-HRP system on a ChemDoc system (Bio-Rad, USA).

Chromatin immunoprecipitation and quantitative PCR

The CDS of *BnaNAC60ΔTM* was constructed into an expression vector pUC19-HF in which a CaMV35S promoter was used to drive the expression of *BnaNAC60ΔTM* tagged with a sequence coding for 3×HA-3×FLAG tag at its 3′ end. ChIP was performed according to (Lee *et al.*, 2017) with minor modifications according to (Saleh *et al.*, 2008). Briefly, 2×10^5 oilseed rape protoplasts were transfected with 20 μg of plasmid DNA and were incubated for 16 h at room temperature before being harvested and washed with 1× PBS buffer (pH 7.4) twice. Samples were cross-linked with 1% formaldehyde in 1× PBS for 10 min at room temperature. Afterwards, glycine (MP Biomedicals) was added at a final concentration of 0.1 M to quench the cross-linking reaction. An anti-HA antibody (Sigma-Aldrich) was used for immunopurification of TF–DNA complexes. A sample without HA antibody was used as the control. Isolated chromatin was sheared by sonication to obtain fragment sizes between 200 and 500 bp. Fragmented genomic DNA was precipitated in the presence of glucogen (Fermentas, USA, https://www.thermofisher.com/). qPCR was performed on the immunoprecipitated DNA on a CFX96 thermocycler. Primers were designed by Primer 3 and the control primers were designed so that the amplified regions were located at least 1 kb away from the ATG translation initiation site. Primers are listed in Table S1. The percentage of genomic DNA precipitated by the anti-HA antibody (ChIP signal) compared with the total input DNA was calculated as follows: percentage of precipitated DNA $= 2^{\Delta(\mathrm{Ct(input)} - \mathrm{Ct(sample)})} \times 100\%$ (Kumar and Lucyshyn, 2017).

Statistical analysis

All the data were generated from three to four biological replicates. Statistical analysis was performed using SPSS (version 16.0, IBM, USA, https://www.ibm.com/products/spss-statistics) software (ANOVA test) and MS Excel 2003 (Student's *t*-test).

ACKNOWLEDGMENTS

We thank Drs. Jorg Kudla (Universität Munster, Germany) for providing the BiFC vectors and Zhi-Zhong Gong (China Agricultural University) for providing C24 seeds. We also thank Moyu Dai and Jiangxiao Zhang (NWAFU) for technical assistance. The work was supported by the National Natural Science Foundation of China (31771699 to YQJ, 31301648 to BY), the Production, Research and Development Program of Yangling (2016CXY-07 to YQJ), the Fundamental Research Funds for the Central Universities (2452017025 to YQJ, 2452019067 to BY), and the Open Project of SKLCSBAA (CSBAA2014004 to JXL).

AUTHOR CONTRIBUTIONS

YQJ and BY conceived and supervised the project. YQJ, BY, and JY designed the experiments. JY, QC, XC, PZ, and SG performed the experiments. TT, PZ, and MKD contributed research materials. JY and YQJ analyzed the data. YQJ, JY, and BY wrote the manuscript. JXL and MKD helped in analyzing the data and writing the manuscript. YQJ, BY, and JXL acquired the funding. All the authors read and approved the manuscript.

CONFLICT OF INTEREST

The authors declare that no competing interests or conflicts of interest exist.

DATA AVAILABILITY STATEMENT

All relevant data can be found within the manuscript and its supporting materials. All the materials described in the paper will be available on request for any non-profit research.

SUPPORTING INFORMATION

Additional Supporting Information may be found in the online version of this article.

Table S1. Primers used in this study.

Figure S1. Multiple alignment analysis of the BnaNAC60 protein with some typical NAC proteins.

Figure S2. Phylogenetic analysis of BnaNAC60 and NTLs from different species.

Figure S3. Subcellullar localization assay of ANAC060 protein in *N. benthamiana*.

Figure S4. Bimolecular fluorescence complementation assay of the interaction between BnaNAC60ΔTM and BnaNAC89ΔTM *in vivo*.

Figure S5. Nuclear relocation of GFP-BnaNAC60 in response to ER stress.

Figure S6. Examination of expression of unfolded protein response marker genes upon ER stress treatment.

Figure S7. Nuclear relocation of GFP-BnaNAC60 in response to oxidative stress.

Figure S8. Expression of *BnaNAC60* induced ROS accumulation and cell death in *N. benthamiana* leaves.

Figure S9. Detection of nuclear DNA fragmentation in leaf tissues expressing *BnaNAC60* via TUNEL assay.

Figure S10. Expression of *ANAC60* from Col-0 does not induce cell death and ROS production in *N. benthamiana* leaves.

Figure S11. Expression of *ANAC060* from C24 fails to induce cell death and ROS production in *N. benthamiana* leaves.

Figure S12. Expression of *ANAC089ΔTM* can induce cell death and ROS production in *N. benthamiana* leaves.

Figure S13. Expression assay of *BnaNAC60ΔTM* in overexpression lines and phenotypic analysis.

Figure S14. Expression of *BnaNAC60* in overexpression lines and leaf senescence phenotypic analysis.

Figure S15. Phenotypic analysis of *BnaNAC60* transgenic plants in dark-induced leaf senescence.

Figure S16. Subcellular localization and immunoblotting analysis of BnaNAC60 in oilseed rape protoplasts.

Figure S17. A dual-luciferase reporter assay of transcriptional control of NACRS elements by BnaNAC60.

Figure S18. Examination of purified GST-BnaNAC60ΔTM protein via SDS-PAGE.

Figure S19. Expression analysis of cell death-, ROS-, and senescence-related marker genes in protoplasts expressing *BnaNAC60* and *BnaNAC60ΔTM*.

Figure S20. qRT-PCR analysis of the expression of ROS-, cell death-, and defense-related marker genes in *N. benthamiana*.

Figure S21. The dual-luciferase reporter assay of transactivation of BnaNAC60 towards two oilseed rape genes.

Figure S22. Competitive EMSA assay of binding of BnaNAC60ΔTM to promoter regions of target genes.

Figure S23. Protein detection and electrophoretic analysis of fragmentated chromatin DNA for ChIP-qPCR assay.

Figure S24. A proposed model of the BnaNAC60 transcription factor in leaf senescence.

Data S1. Materials and methods.

REFERENCES

Aoyagi, S., Sugiyama, M. and Fukuda, H. (1998) BEN1 and ZEN1 cDNAs encoding S1-type DNases that are associated with programmed cell death in plants. *FEBS Lett.* **429**, 134–138.

Balazadeh, S., Kwasniewski, M., Caldana, C., Mehrnia, M., Zanor, M.I., Xue, G.P. and Mueller-Roeber, B. (2011) ORS1, an H_2O_2 - responsive NAC transcription factor, controls senescence in Arabidopsis thaliana. *Mol. Plant*, **4**, 346–360.

Balazadeh, S., Riano-Pachon, D.M. and Mueller-Roeber, B. (2008) Transcription factors regulating leaf senescence in Arabidopsis thaliana. *Plant Biol.* **10**(Suppl 1), 63–75.

Balazadeh, S., Siddiqui, H., Allu, A.D., Matallana-Ramirez, L.P., Caldana, C., Mehrnia, M., Zanor, M.I., Kohler, B. and Mueller-Roeber, B. (2010) A gene regulatory network controlled by the NAC transcription factor ANAC092/AtNAC2/ORE1 during salt-promoted senescence. *Plant J.* **62**, 250–264.

Bowman, J.L., Floyd, S.K. and Sakakibara, K. (2007) Green genes-comparative genomics of the green branch of life. *Cell*, **129**, 229–234.

Buono, R.A., Hudecek, R. and Nowack, M.K. (2019) Plant proteases during developmental programmed cell death. *J. Exp. Bot.* **70**, 2097–2112.

Chen, B., Niu, F., Liu, W.Z., Yang, B., Zhang, J., Ma, J., Cheng, H., Han, F. and Jiang, Y.Q. (2016) Identification, cloning and characterization of R2R3-MYB gene family in canola (*Brassica napus* L.) identify a novel member modulating ROS accumulation and hypersensitive-like cell death. *DNA Res.* **23**, 101–114.

Chen, X., Truksa, M., Shah, S. and Weselake, R.J. (2010) A survey of quantitative real-time polymerase chain reaction internal reference genes for expression studies in *Brassica napus*. *Anal. Biochem.* **405**, 138–140.

Chen, Y.N., Slabaugh, E. and Brandizzi, F. (2008) Membrane-tethered transcription factors in Arabidopsis thaliana: novel regulators in stress response and development. *Curr. Opin. Plant Biol.* **11**, 695–701.

Clough, S.J. and Bent, A.F. (1998) Floral dip: a simplified method for Agrobacterium-mediated transformation of *Arabidopsis thaliana*. *Plant J.* **16**, 735–743.

Czechowski, T., Stitt, M., Altmann, T., Udvardi, M.K. and Scheible, W.R. (2005) Genome-wide identification and testing of superior reference genes for transcript normalization in Arabidopsis. *Plant Physiol.* **139**, 5–17.

Daneva, A., Gao, Z., Van Durme, M. and Nowack, M.K. (2016) Functions and regulation of programmed cell death in plant development. *Annu. Rev. Cell Dev. Biol.* **32**, 441–468.

Davletova, S., Schlauch, K., Coutu, J. and Mittler, R. (2005) The zinc-finger protein Zat12 plays a central role in reactive oxygen and abiotic stress signaling in Arabidopsis. *Plant Physiol.* **139**, 847–856.

De Clercq, I., Vermeirssen, V., Van Aken, O. *et al.* (2013) The membrane-bound NAC transcription factor ANAC013 functions in mitochondrial retrograde regulation of the oxidative stress response in Arabidopsis. *Plant Cell*, **25**, 3472–3490.

Epple, P., Mack, A.A., Morris, V.R. and Dangl, J.L. (2003) Antagonistic control of oxidative stress-induced cell death in Arabidopsis by two related, plant-specific zinc finger proteins. *Proc. Natl Acad. Sci. USA*, **100**, 6831–6836.

Fan, Z.Q., Tan, X.L., Chen, J.W., Liu, Z.L., Kuang, J.F., Lu, W.J., Shan, W. and Chen, J.Y. (2018) BrNAC055, a novel transcriptional activator, regulates leaf senescence in Chinese flowering cabbage by modulating reactive oxygen species production and chlorophyll degradation. *J. Agric. Food Chem.* **66**, 9399–9408.

Farage-Barhom, S., Burd, S., Sonego, L., Perl-Treves, R. and Lers, A. (2008) Expression analysis of the BFN1 nuclease gene promoter during senescence, abscission, and programmed cell death-related processes. *J. Exp. Bot.* **59**, 3247–3258.

Gan, S. and Amasino, R.M. (1997) Making sense of senescence (molecular genetic regulation and manipulation of leaf senescence). *Plant Physiol.* **113**, 313–319.

Gepstein, S., Sabehi, G., Carp, M.J., Hajouj, T., Nesher, M.F., Yariv, I., Dor, C. and Bassani, M. (2003) Large-scale identification of leaf senescence-associated genes. *Plant J.* **36**, 629–642.

Guo, Y., Cai, Z. and Gan, S. (2004) Transcriptome of Arabidopsis leaf senescence. *Plant Cell Environ.* **27**, 521–549.

Guo, Y. and Gan, S. (2006) AtNAP, a NAC family transcription factor, has an important role in leaf senescence. *Plant J.* **46**, 601–612.

Guo, Y. and Gan, S.S. (2012) Convergence and divergence in gene expression profiles induced by leaf senescence and 27 senescence-promoting hormonal, pathological and environmental stress treatments. *Plant Cell Environ.* **35**, 644–655.

Hara-Nishimura, I., Hatsugai, N., Nakaune, S., Kuroyanagi, M. and Nishimura, M. (2005) Vacuolar processing enzyme: an executor of plant cell death. *Curr. Opin. Plant Biol.* **8**, 404–408.

Hatsugai, N., Kuroyanagi, M., Yamada, K., Meshi, T., Tsuda, S., Kondo, M., Nishimura, M. and Hara-Nishimura, I. (2004) A plant vacuolar protease, VPE, mediates virus-induced hypersensitive cell death. *Science*, **305**, 855–858.

Hatsugai, N., Yamada, K., Goto-Yamada, S. and Hara-Nishimura, I. (2015) Vacuolar processing enzyme in plant programmed cell death. *Front. Plant Sci.* **6**, 234.

He, Y. and Gan, S. (2002) A gene encoding an acyl hydrolase is involved in leaf senescence in Arabidopsis. *Plant Cell*, **14**, 805–815.

Heath, M.C. (2000) Hypersensitive response-related death. *Plant Mol. Biol.* **44**, 321–334.

Hellens, R.P., Allan, A.C., Friel, E.N., Bolitho, K., Grafton, K., Templeton, M.D., Karunairetnam, S., Gleave, A.P. and Laing, W.A. (2005) Transient expression vectors for functional genomics, quantification of promoter activity and RNA silencing in plants. *Plant Methods*, **1**, 13.

Horie, Y., Ito, H., Kusaba, M., Tanaka, R. and Tanaka, A. (2009) Participation of chlorophyll b reductase in the initial step of the degradation of light-harvesting chlorophyll a/b-protein complexes in Arabidopsis. *J. Biol. Chem.* **284**, 17449–17456.

Hortensteiner, S. (2006) Chlorophyll degradation during senescence. *Annu. Rev. Plant Biol.* **57**, 55–77.

Hortensteiner, S. and Krautler, B. (2011) Chlorophyll breakdown in higher plants. *Biochim. Biophys. Acta*, **1807**, 977–988.

Ito, J. and Fukuda, H. (2002) ZEN1 is a key enzyme in the degradation of nuclear DNA during programmed cell death of tracheary elements. *Plant Cell*, **14**, 3201–3211.

James, M., Poret, M., Masclaux-Daubresse, C., Marmagne, A., Coquet, L., Jouenne, T., Chan, P., Trouverie, J. and Etienne, P. (2018) SAG12, a major cysteine protease involved in nitrogen mobilization during senescence for seed production in Arabidopsis thaliana. *Plant Cell Physiol.* **59**, 2052–2063.

Kadota, Y., Shirasu, K. and Zipfel, C. (2015) Regulation of the NADPH oxidase RBOHD during plant immunity. *Plant Cell Physiol.* **56**, 1472–1480.

Kaneda, T., Taga, Y., Takai, R., Iwano, M., Matsui, H., Takayama, S., Isogai, A. and Che, F.S. (2009) The transcription factor OsNAC4 is a key positive regulator of plant hypersensitive cell death. *EMBO J.* **28**, 926–936.

Khanna-Chopra, R. (2012) Leaf senescence and abiotic stresses share reactive oxygen species-mediated chloroplast degradation. *Protoplasma*, **249**, 469–481.

Kim, H.J., Nam, H.G. and Lim, P.O. (2016) Regulatory network of NAC transcription factors in leaf senescence. *Curr. Opin. Plant Biol.* **33**, 48–56.

Kim, M.J., Park, M.J., Seo, P.J., Song, J.S., Kim, H.J. and Park, C.M. (2012) Controlled nuclear import of the transcription factor NTL6 reveals a cytoplasmic role of SnRK2.8 in the drought-stress response. *Biochem. J.* **448**, 353–363.

Kim, S.G., Lee, S., Ryu, J. and Park, C.M. (2010a) Probing protein structural requirements for activation of membrane-bound NAC transcription factors in Arabidopsis and rice. *Plant Sci.* **178**, 239–244.

Kim, S.G., Lee, S., Seo, P.J., Kim, S.K., Kim, J.K. and Park, C.M. (2010b) Genome-scale screening and molecular characterization of membrane-bound transcription factors in Arabidopsis and rice. *Genomics*, **95**, 56–65.

Kim, S.Y., Kim, S.G., Kim, Y.S., Seo, P.J., Bae, M., Yoon, H.K. and Park, C.M. (2007) Exploring membrane-associated NAC transcription factors in Arabidopsis: implications for membrane biology in genome regulation. *Nucleic Acids Res.* **35**, 203–213.

Kim, Y.S., Kim, S.G., Park, J.E., Park, H.Y., Lim, M.H., Chua, N.H. and Park, C.M. (2006) A membrane-bound NAC transcription factor regulates cell division in Arabidopsis. *Plant Cell*, **18**, 3132–3144.

Kim, Y.S., Sakuraba, Y., Han, S.H., Yoo, S.C. and Paek, N.C. (2013) Mutation of the Arabidopsis NAC016 transcription factor delays leaf senescence. *Plant Cell Physiol.* **54**, 1660–1672.

Kumar, S.V. and Lucyshyn, D. (2017) Studying transcription factor binding to specific genomic loci by chromatin immunoprecipitation (ChIP). *Methods Mol. Biol.* **1497**, 193–203.

Le, D.T., Nishiyama, R., Watanabe, Y., Mochida, K., Yamaguchi-Shinozaki, K., Shinozaki, K. and Tran, L.S. (2011) Genome-wide survey and expression analysis of the plant-specific NAC transcription factor family in soybean during development and dehydration stress. *DNA Res.* **18**, 263–276.

Lee, J.H., Jin, S., Kim, S.Y., Kim, W. and Ahn, J.H. (2017) A fast, efficient chromatin immunoprecipitation method for studying protein-DNA binding in Arabidopsis mesophyll protoplasts. *Plant Methods*, **13**, 42.

Lee, S., Seo, P.J., Lee, H.J. and Park, C.M. (2012) A NAC transcription factor NTL4 promotes reactive oxygen species production during drought-induced leaf senescence in Arabidopsis. *Plant J.* **70**, 831–844.

Li, J., Zhang, J., Wang, X. and Chen, J. (2010) A membrane-tethered transcription factor ANAC089 negatively regulates floral initiation in Arabidopsis thaliana. *Sci. China Life Sci.* **53**, 1299–1306.

Li, P., Zhou, H., Shi, X. *et al.* (2014) The ABI4-induced Arabidopsis ANAC060 transcription factor attenuates ABA signaling and renders seedlings sugar insensitive when present in the nucleus. *PLoS Genet.* **10**, e1004213.

Liang, C., Wang, Y., Zhu, Y. *et al.* (2014) OsNAP connects abscisic acid and leaf senescence by fine-tuning abscisic acid biosynthesis and directly targeting senescence-associated genes in rice. *Proc. Natl Acad. Sci. USA*, **111**, 10013–10018.

Liang, M., Li, H., Zhou, F., Li, H., Liu, J., Hao, Y., Wang, Y., Zhao, H. and Han, S. (2015) Subcellular distribution of NTL transcription factors in Arabidopsis thaliana. *Traffic*, **16**, 1062–1074.

Lim, P.O., Kim, H.J. and Nam, H.G. (2007) Leaf senescence. *Annu. Rev. Plant Biol.* **58**, 115–136.

Lindemose, S., Jensen, M.K., Van de Velde, J., O'Shea, C., Heyndrickx, K.S., Workman, C.T., Vandepoele, K., Skriver, K. and De Masi, F. (2014) A DNA-binding-site landscape and regulatory network analysis for NAC transcription factors in Arabidopsis thaliana. *Nucleic Acids Res.* **42**, 7681–7693.

Ma, X., Zhang, Y., Tureckova, V., Xue, G.P., Fernie, A.R., Mueller-Roeber, B. and Balazadeh, S. (2018) The NAC transcription factor SINAP2 regulates leaf senescence and fruit yield in tomato. *Plant Physiol.* **177**, 1286–1302.

Mahmood, K., El-Kereamy, A., Kim, S.H., Nambara, E. and Rothstein, S.J. (2016) ANAC032 positively regulates age-dependent and stress-induced senescence in Arabidopsis thaliana. *Plant Cell Physiol.* **57**, 2029–2046.

Mao, C., Lu, S., Lv, B., Zhang, B., Shen, J., He, J., Luo, L., Xi, D., Chen, X. and Ming, F. (2017) A rice NAC transcription factor promotes leaf senescence via ABA biosynthesis. *Plant Physiol.* **174**, 1747–1763.

Marino, D., Dunand, C., Puppo, A. and Pauly, N. (2012) A burst of plant NADPH oxidases. *Trends Plant Sci.* **17**, 9–15.

Matallana-Ramirez, L.P., Rauf, M., Farage-Barhom, S., Dortay, H., Xue, G.P., Droge-Laser, W., Lers, A., Balazadeh, S. and Mueller-Roeber, B. (2013) NAC transcription factor ORE1 and senescence-induced bifunctional nuclease1 (BFN1) constitute a regulatory cascade in Arabidopsis. *Mol. Plant*, **6**, 1432–1452.

Mendes, G.C., Reis, P.A., Calil, I.P., Carvalho, H.H., Aragao, F.J. and Fontes, E.P. (2013) GmNAC30 and GmNAC81 integrate the endoplasmic reticulum stress- and osmotic stress-induced cell death responses through a vacuolar processing enzyme. *Proc. Natl Acad. Sci. USA*, **110**, 19627–19632.

Mhamdi, A. and Van Breusegem, F. (2018) Reactive oxygen species in plant development. *Development*, **145**, dev164376.

Mittler, R. (2017) ROS are good. *Trends Plant Sci.* **22**, 11–19.

Nelson, B.K., Cai, X. and Nebenfuhr, A. (2007) A multicolored set of in vivo organelle markers for co-localization studies in Arabidopsis and other plants. *Plant J.* **51**, 1126–1136.

Ng, S., Ivanova, A., Duncan, O. *et al.* (2013) A membrane-bound NAC transcription factor, ANAC017, mediates mitochondrial retrograde signaling in Arabidopsis. *Plant Cell*, **25**, 3450–3471.

Oda-Yamamizo, C., Mitsuda, N., Sakamoto, S., Ogawa, D., Ohme-Takagi, M. and Ohmiya, A. (2016) The NAC transcription factor ANAC046 is a positive regulator of chlorophyll degradation and senescence in Arabidopsis leaves. *Sci. Rep.* **6**, 23609.

Olsen, A.N., Ernst, H.A., Leggio, L.L. and Skriver, K. (2005) NAC transcription factors: structurally distinct, functionally diverse. *Trends Plant Sci.* **10**, 79–87.

Park, J., Kim, Y.S., Kim, S.G., Jung, J.H., Woo, J.C. and Park, C.M. (2011) Integration of auxin and salt signals by the NAC transcription factor NTM2 during seed germination in Arabidopsis. *Plant Physiol.* **156**, 537–549.

Patterson, B.D., MacRae, E.A. and Ferguson, I.B. (1984) Estimation of hydrogen peroxide in plant extracts using titanium(IV). *Anal. Biochem.* **139**, 487–492.

Perez-Amador, M.A., Abler, M.L., De Rocher, E.J., Thompson, D.M., van Hoof, A., LeBrasseur, N.D., Lers, A. and Green, P.J. (2000) Identification of BFN1, a bifunctional nuclease induced during leaf and stem senescence in Arabidopsis. *Plant Physiol.* **122**, 169–180.

Pfaffl, M.W. (2001) A new mathematical model for relative quantification in real-time RT-PCR. *Nucleic Acids Res.* **29**, e45.

Pimenta, M.R., Silva, P.A., Mendes, G.C. *et al.* (2016) The stress-induced Soybean NAC transcription factor GmNAC81 plays a positive role in developmentally programmed leaf senescence. *Plant Cell Physiol.* **57**, 1098–1114.

Pontier, D., Gan, S., Amasino, R.M., Roby, D. and Lam, E. (1999) Markers for hypersensitive response and senescence show distinct patterns of expression. *Plant Mol. Biol.* **39**, 1243–1255.

Puranik, S., Sahu, P.P., Srivastava, P.S. and Prasad, M. (2012) NAC proteins: regulation and role in stress tolerance. *Trends Plant Sci.* **17**, 369–381.

Qiu, K., Li, Z., Yang, Z. *et al.* (2015) EIN3 and ORE1 accelerate degreening during ethylene-mediated leaf senescence by directly activating chlorophyll catabolic genes in Arabidopsis. *PLoS Genet.* **11**, e1005399.

Rauf, M., Arif, M., Dortay, H., Matallana-Ramirez, L.P., Waters, M.T., Gil Nam, H., Lim, P.O., Mueller-Roeber, B. and Balazadeh, S. (2013) ORE1 balances leaf senescence against maintenance by antagonizing G2-like-mediated transcription. *EMBO Rep.* **14**, 382–388.

Rivero, R.M., Kojima, M., Gepstein, A., Sakakibara, H., Mittler, R., Gepstein, S. and Blumwald, E. (2007) Delayed leaf senescence induces extreme drought tolerance in a flowering plant. *Proc. Natl Acad. Sci. USA*, **104**, 19631–19636.

Rizhsky, L., Davletova, S., Liang, H. and Mittler, R. (2004) The zinc finger protein Zat12 is required for cytosolic ascorbate peroxidase 1 expression during oxidative stress in Arabidopsis. *J. Biol. Chem.* **279**, 11736–11743.

Rogers, H. and Munne-Bosch, S. (2016) Production and scavenging of reactive oxygen species and redox signaling during leaf and flower senescence: similar but different. *Plant Physiol.* **171**, 1560–1568.

Sakuraba, Y., Han, S.H., Lee, S.H., Hortensteiner, S. and Paek, N.C. (2016) Arabidopsis NAC016 promotes chlorophyll breakdown by directly upregulating STAYGREEN1 transcription. *Plant Cell Rep.* **35**, 155–166.

Sakuraba, Y., Kim, Y.S., Han, S.H., Lee, B.D. and Paek, N.C. (2015) The Arabidopsis transcription factor NAC016 promotes drought stress responses by repressing AREB1 transcription through a trifurcate feed-forward regulatory loop involving NAP. *Plant Cell*, **27**, 1771–1787.

Saleh, A., Alvarez-Venegas, R. and Avramova, Z. (2008) An efficient chromatin immunoprecipitation (ChIP) protocol for studying histone modifications in Arabidopsis plants. *Nat. Protoc.* **3**, 1018–1025.

Sato, Y., Morita, R., Katsuma, S., Nishimura, M., Tanaka, A. and Kusaba, M. (2009) Two short-chain dehydrogenase/reductases, NON-YELLOW COLORING 1 and NYC1-LIKE, are required for chlorophyll b and light-harvesting complex II degradation during senescence in rice. *Plant J.* **57**, 120–131.

Seo, P.J., Kim, M.J., Park, J.Y., Kim, S.Y., Jeon, J., Lee, Y.H., Kim, J. and Park, C.M. (2010) Cold activation of a plasma membrane-tethered NAC transcription factor induces a pathogen resistance response in Arabidopsis. *Plant J.* **61**, 661–671.

Seo, P.J., Kim, S.G. and Park, C.M. (2008) Membrane-bound transcription factors in plants. *Trends Plant Sci.* **13**, 550–556.

Seo, P.J., Park, J.M., Kang, S.K., Kim, S.G. and Park, C.M. (2011) An Arabidopsis senescence-associated protein SAG29 regulates cell viability under high salinity. *Planta*, **233**, 189–200.

Sun, Y., Wang, C., Yang, B. *et al.* (2014) Identification and functional analysis of mitogen-activated protein kinase kinase kinase (MAPKKK) genes in canola (Brassica napus L.). *J. Exp. Bot.* **65**, 2171–2188.

Suzuki, N., Miller, G., Morales, J., Shulaev, V., Torres, M.A. and Mittler, R. (2011) Respiratory burst oxidases: the engines of ROS signaling. *Curr. Opin. Plant Biol.* **14**, 691–699.

Thomas, H. (2013) Senescence, ageing and death of the whole plant. *New Phytol.* **197**, 696–711.

Torres, M.A., Dangl, J.L. and Jones, J.D. (2002) Arabidopsis gp91phox homologues AtrbohD and AtrbohF are required for accumulation of reactive oxygen intermediates in the plant defense response. *Proc. Natl Acad. Sci. USA*, **99**, 517–522.

Uauy, C., Distelfeld, A., Fahima, T., Blechl, A. and Dubcovsky, J. (2006) A NAC gene regulating senescence improves grain protein, zinc, and iron content in wheat. *Science*, **314**, 1298–1301.

Van Aken, O. and Pogson, B.J. (2017) Convergence of mitochondrial and chloroplastic ANAC017/PAP-dependent retrograde signalling pathways and suppression of programmed cell death. *Cell Death Differ.* **24**, 955–960.

Wang, B., Guo, X., Wang, C., Ma, J., Niu, F., Zhang, H., Yang, B., Liang, W., Han, F. and Jiang, Y.Q. (2015) Identification and characterization of plant-specific NAC gene family in canola (*Brassica napus* L.) reveal novel members involved in cell death. *Plant Mol. Biol.* **87**, 395–411.

Waters, M.T., Moylan, E.C. and Langdale, J.A. (2008) GLK transcription factors regulate chloroplast development in a cell-autonomous manner. *Plant J.* **56**, 432–444.

Weaver, L.M., Gan, S., Quirino, B. and Amasino, R.M. (1998) A comparison of the expression patterns of several senescence-associated genes in response to stress and hormone treatment. *Plant Mol. Biol.* **37**, 455–469.

Woo, H.R., Kim, H.J., Nam, H.G. and Lim, P.O. (2013) Plant leaf senescence and death - regulation by multiple layers of control and implications for aging in general. *J. Cell Sci.* **126**, 4823–4833.

Woo, H.R., Koo, H.J., Kim, J. *et al.* (2016) Programming of plant leaf senescence with temporal and inter-organellar coordination of transcriptome in Arabidopsis. *Plant Physiol.* **171**, 452–467.

Wu, A., Allu, A.D., Garapati, P. *et al.* (2012) JUNGBRUNNEN1, a reactive oxygen species-responsive NAC transcription factor, regulates longevity in Arabidopsis. *Plant Cell*, **24**, 482–506.

Yan, J., Tong, T., Li, X., Chen, Q., Dai, M., Niu, F., Yang, M., Deyholos, M.K., Yang, B. and Jiang, Y.Q. (2018) A novel NAC-type transcription factor, NAC87, from oilseed rape modulates reactive oxygen species accumulation and cell death. *Plant Cell Physiol.* **59**, 290–303.

Yang, L., Ye, C., Zhao, Y., Cheng, X., Wang, Y., Jiang, Y.Q. and Yang, B. (2018) An oilseed rape WRKY-type transcription factor regulates ROS accumulation and leaf senescence in *Nicotiana benthamiana* and Arabidopsis through modulating transcription of RbohD and RbohF. *Planta*, **247**, 1323–1338.

Yang, S.D., Seo, P.J., Yoon, H.K. and Park, C.M. (2011) The Arabidopsis NAC transcription factor VNI2 integrates abscisic acid signals into leaf senescence via the COR/RD genes. *Plant Cell*, **23**, 2155–2168.

Yang, Z.T., Lu, S.J., Wang, M.J., Bi, D.L., Sun, L., Zhou, S.F., Song, Z.T. and Liu, J.X. (2014a) A plasma membrane-tethered transcription factor, NAC062/ANAC062/NTL6, mediates the unfolded protein response in Arabidopsis. *Plant J.* **79**, 1033–1043.

Yang, Z.T., Wang, M.J., Sun, L., Lu, S.J., Bi, D.L., Sun, L., Song, Z.T., Zhang, S.S., Zhou, S.F. and Liu, J.X. (2014b) The membrane-associated transcription factor NAC089 controls ER-stress-induced programmed cell death in plants. *PLoS Genet.* **10**, e1004243.

Yoo, S.D., Cho, Y.H. and Sheen, J. (2007) Arabidopsis mesophyll protoplasts: a versatile cell system for transient gene expression analysis. *Nat. Protoc.* **2**, 1565–1572.

Zhang, D., Liu, D., Lv, X., Wang, Y., Xun, Z., Liu, Z., Li, F. and Lu, H. (2014) The cysteine protease CEP1, a key executor involved in tapetal programmed cell death, regulates pollen development in Arabidopsis. *Plant Cell*, **26**, 2939–2961.

Zhang, K. and Gan, S.S. (2012) An abscisic acid-AtNAP transcription factor-SAG113 protein phosphatase 2C regulatory chain for controlling dehydration in senescing Arabidopsis leaves. *Plant Physiol.* **158**, 961–969.

Zheng, M.S., Takahashi, H., Miyazaki, A., Hamamoto, H., Shah, J., Yamaguchi, I. and Kusano, T. (2004) Up-regulation of Arabidopsis thaliana NHL10 in the hypersensitive response to Cucumber mosaic virus infection and in senescing leaves is controlled by signalling pathways that differ in salicylate involvement. *Planta*, **218**, 740–750.

Zhu, X., Chen, J., Xie, Z., Gao, J., Ren, G., Gao, S., Zhou, X. and Kuai, B. (2015) Jasmonic acid promotes degreening via MYC2/3/4- and ANAC019/055/072-mediated regulation of major chlorophyll catabolic genes. *Plant J.* **84**, 597–610.